NPS-62OL76102

NAVAL POSTGRADUATE SCHOOL

Monterey, California

BIT ERROR RATE MEASUREMENTS
ON THE AN/WSC-3 AND AN/SSR-1
SATELLITE COMMUNICATIONS SETS

Richard F. Carlson
John E. Ohlson

October 1976

Approved for Public Release: Distribution unlimited
A task under the Shipboard RFI in UHF SATCOM Project
Prepared for:
Naval Electronic Systems Command
PME 106
Washington, D.C. 20360

NAVAL POSTGRADUATE SCHOOL
Monterey, California

Rear Admiral Isham Linder
Superintendent
15 October 1976

Jack R. Borsting
Provost

ABSTRACT

The purpose of this investigation is to characterize the performance of the AN/WSC-3 and AN/SSR-1 satellite communications sets. The characterization considered in this report is probability of error. The receivers' performance to random uncoded data is measured and compared to their theoretical performance.

SECURITY CLASSIFICATION OF THIS PAGE *(When Data Entered)*

REPORT DOCUMENTATION PAGE

READ INSTRUCTIONS BEFORE COMPLETING FORM

1. REPORT NUMBER: NPS-620L76102	2. GOVT ACCESSION NO.
3. RECIPIENT'S CATALOG NUMBER	
4. TITLE *(and Subtitle)*: BIT ERROR RATE MEASUREMENTS ON THE AN/WSC-3 and AN/SSR-1 SATELLITE COMMUNICATIONS SETS	5. TYPE OF REPORT & PERIOD COVERED: Task Report
	6. PERFORMING ORG. REPORT NUMBER
7. AUTHOR(s): Richard F. Carlson, John E. Ohlson	8. CONTRACT OR GRANT NUMBER(s): N00039 76 WRT 9053
9. PERFORMING ORGANIZATION NAME AND ADDRESS: Naval Postgraduate School, Monterey, California 93940	10. PROGRAM ELEMENT, PROJECT, TASK AREA & WORK UNIT NUMBERS
11. CONTROLLING OFFICE NAME AND ADDRESS: Naval Electronics Systems Command, PME-106, Washington, D.C. 20360	12. REPORT DATE: October 1976
	13. NUMBER OF PAGES: 60
14. MONITORING AGENCY NAME & ADDRESS *(if different from Controlling Office)*	15. SECURITY CLASS. *(of this report)*: UNCLASSIFIED
	15a. DECLASSIFICATION/DOWNGRADING SCHEDULE

16 DISTRIBUTION STATEMENT *(of this Report)*

Approved for public release: Distribution unlimited

17. DISTRIBUTION STATEMENT *(of the abstract entered in Block 20, if different from Report)*

18. SUPPLEMENTARY NOTES

19. KEY WORDS *(Continue on reverse side if necessary and identify by block number)*

RFI
SATCOM
BIT ERROR RATE

20. ABSTRACT *(Continue on reverse side if necessary and identify by block number)*

The purpose of this investigation is to characterize the performance of the AN/WSC-3 and the AN/SSR-1 satellite communications sets. The characterization considered in this report is probability of error. The receivers' performance to random uncoded data is measured and compared to their theoretical performance.

DD FORM 1 JAN 73 1473 EDITION OF 1 NOV 65 IS OBSOLETE
S/N 0102-014-6601

UNCLASSIFIED
SECURITY CLASSIFICATION OF THIS PAGE *(When Data Entered)*

TABLE OF CONTENTS

LIST OF FIGURES

LIST OF TABLES

I. INTRODUCTION

The best overall evaluation of the performance of a communication system is a quantitative evaluation of the quality of its output. In a digital communication system this evaluation naturally takes the form of a comparison of transmitted data to demodulated data. The quantitative measurement of this is termed bit error rate.

For the purposes of this report the transmitted data is a differentially encoded phase shift keyed waveform. Thus the source alphabet contains two characters referred to as "1" and "0". It is assumed that each baud has an energy content equal to any other baud and

$$s_0(t) = A \cos \omega_0 t$$

$$s_1(t) = -A \cos \omega_0 t$$

so that $s_0(t) = -s_1(t)$. It is assumed that the signals are equally likely.

The event of an error in the demodulated data is the event of a source character being received as another source character. For the two letter alphabet considered, the probability of error is

$$P_e = P(\text{"1" received/"0"transmitted})P(\text{"0"transmitted}) + P(\text{"0"received/"1"transmitted})P(\text{"1"transmitted})$$

or

$$P_e = 1/2\{P(\text{"1"/"0"}) + P(\text{"0"/"1"})\}$$

since P("1") = P("0") = 1/2.

It is known [1] the best decision between "0" and "1" from the waveforms $s_0(t)$ and $s_1(t)$ embedded in gaussian noise and defined over a baud length T_0 consists of two matched filters, one matched to s_0 and the other matched to s_1.

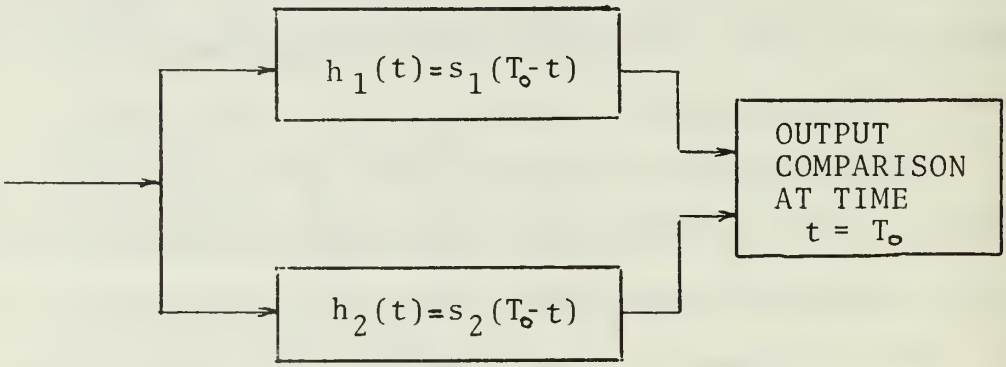

For antipodal signals only one matched filter is required and the output is fed to a "greater or less than zero" threshold. A well known result for PSK waveforms detected in this manner is [2].

$$P_{e(PSK)} = \text{erfc } \sqrt{2E_b/N_0}$$

Where E_b is the bit energy defined over a single baud, N_0 is noise power density and erfc is the complementary error function defined as

$$\text{erfc}[x] = \int_x^\infty \frac{e^{-y^2/2}}{\sqrt{2\pi}}\, dy$$

Integrate and dump after coherent detection (using a phase locked loop) is usually done rather than using a matched filter.

It is necessary to consider the effect of differential encoding of the transmitted data and the modification necessary to the previous discussion on the error probability of the decoded data.

Differential encoding of a data stream of "0"'s and "1"'s can be defined as follows:

A "1" causes a 180 degree phase change in the transmitted data stream,

A "0" causes no phase change in the transmitted data stream.

Decoding the differentially encoded data stream simply involves the pairwise EXCLUSIVE-ORing of adjacent bands. There are two methods of accomplishing this. The first method is termed differentially coherent PSK or DPSK and compares successive bauds only. For DPSK the probability of error is given by [2]

$$P_{e(DPSK)} = \frac{1}{2} e^{-E_b/N_0}$$

A second technique is termed coherent differential PSK or CPSK and does a coherent detection using a phase reference derived from many previous bauds.

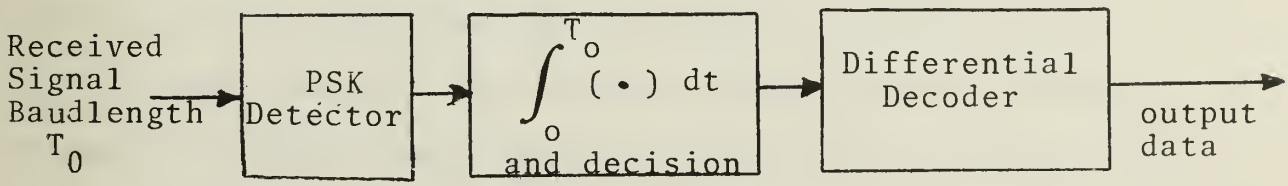

The DPSK technique is generally not used in SATCOM because there is no easily provided technique of frequency tracking.

The CPSK method utilizes a PSK demodulator and then differentially decodes the demodulated data stream. Each detected but not decoded baud has a probability of error as given previously for PSK. An error in the decoded data stream is seen to occur if only one of the paired bauds in the encoded data is in error. If both bauds are in error the result will be a correct decoding. Thus,

$$P_{e(CPSK)} = P \text{ (first baud in pair in error and second baud is not in error)} + P \text{ (first baud in pair not in error and the second baud in error).}$$

Let P(first baud in error) = P(second baud in error) = p

then

$$P_{e(CPSK)} = p(1-p) + p(1-p)$$

$$= 2p(1-p)$$

where $p = P_{e(PSK)}$. Thus assuming the phase locked loop to have zero phase error

$$P_{e(CPSK)} = 2\text{erfc}\sqrt{\frac{2E_b}{N_0}}\left[1 - \text{erfc}\sqrt{\frac{2E_b}{N_0}}\right]$$

The AN/WSC-3 and AN/SSR-1 satellite communications units use the CPSK technique.

The relation obtained for CPSK has an interesting property. For high signal-to-noise ratio and low probability of bit error, P_e is approximated by simply 2p indicating errors will tend to occur in pairs. This has been verified by laboratory observation.

The term E_b/N_0 which appears in all the probability of error expressions can be considered a signal-to-noise ratio in a bandwidth equal to the data rate.

$$E_b/N_0 = ST_0/kT_s = S/kT_sR$$

where E_b is the signal energy in a baud of length T_0, S is the signal power, R is the data rate, T_s is the receiver system noise temperature, and k is Boltzmann's constant equal to -228.6 dBW/Hz-K.

In experimentally measuring bit error rate it is desired to obtain two estimates. First a point estimate of the error rate and second an interval estimate of the error rate or confidence interval.

The best point estimate of the error rate, $\hat{p}$, is defined as the unbiased estimate that has a smaller variance than any other estimate. A necessary assumption is that the error rate is constant and the trials are independent.

Crow [3] has considered various techniques of sampling and their associated distributions. If the sample size, n, is prescribed then the number of errors ("successes"), c, is given by the binomial distribution and $\hat{p}$ is chosen as

$$\hat{p} = c/n$$

Then $\hat{p}$ is unbiased

$$E[\hat{p}] = E[c/n] = \frac{(np)}{n} = p$$

where $E[\bullet]$ is expectation. The estimate, $\hat{p}$, is also the maximum likelihood estimate. For np large a gaussian approximation to the distribution may be used although Crow noted that for large n and small p as commonly found in digital communication error rates a poisson approximation results in a smaller interval estimate.

An interval estimate of p is the estimate of an interval which will cover p with an arbitrarily selected probability called a confidence coefficient, Z(k), where k is a confidence parameter. With the assumptions of E[c] = np and

$\sigma_c^2 = np(1-p) \doteq np \doteq n\hat{p}$ so that $\sigma_c = \sqrt{c}$ it is easily shown that

$$Z(k) = P\left[\hat{p}\left(1 - \frac{k}{\sqrt{c}}\right) < p < \hat{p}\left(1 + \frac{k}{\sqrt{c}}\right)\right]$$

where Z(k) and k are determined from normal distribution tables. For example

Z(k)	k(PSK)	k(CPSK)
.50	.6745	.9539
.80	1.2816	1.8125
.90	1.6449	2.3262
.95	1.9600	2.7719
.99	2.5757	3.6426

In the case of CPSK, $\sigma_c = \sqrt{2c}$ because of errors occurring in pairs. It is important to note that the confidence interval is reduced by larger c, the number of counted errors.

If samples are taken until a predetermined number of successes occur then the number of trials becomes a random variable. This situation is governed by the inverse binomial distribution

$$P = \binom{n-1}{c-1} p^c (1-p)^{n-c}$$

The nth trial results in an error with probability p and the other c-1 errors may occur in any of the other n-1 trials. In this case a suitable estimate of p is

$$\hat{p} = \frac{c-1}{n-1}$$

Crow [3] notes that the lower confidence bound may be determined as in binomial sampling with c successes in n trials but the upper confidence limit must be determined as binomial with c-1 successes in n-1 trials.

If the confidence intervals for the binomial sampling are applied to the case of inverse binomial sampling the effect would be to increase the probability of covering p in the confidence interval beyond that required. This has been verified by Crow in Monte Carlo simulation.

The data in this report were taken with the requirement of measuring a large c. Thus the question of data confidence limits has been minimized. However in other work with various interferers, not reported here, consideration of confidence limits is desirable and necessary.

Noise figure will be an important parameter in later discussions concerning the sensitivity of the receivers and in the reduction of bit error rate measurements to E_b/N_0 as previously noted. Noise figure, usually expressed in dB, is derived from the more fundamental quantity, system noise temperature, as follows:

$$F = 1 + T_s/290$$

System noise temperature is found by summing the individual system element noise temperatures divided by the gain of all elements that precede them.

II. AN/WSC-3 MEASUREMENTS

The experimental setup configuration used for obtaining bit error rate data for the AN/WSC-3 satellite communications unit is shown in Figure 1.

Since in the laboratory configuration the AN/WSC-3 and its preamplifier-diplexer, the AM-6691, were located physically next to each other an attenuation of 2.8 dB was placed between them to simulate a typical shipboard cable run. The transmission line between the AN/WSC-3 and the AM-6691 in a shipboard installation is air dielectric coaxial RG-318/U with an attenuation at the frequencies of interest of 0.7 dB per 100 feet. Thus an approximate cable run of 400 feet was simulated in this manner.

The HP-1645A Data Error Analyzer generates a selectable length linear maximal pseudorandum sequence with TTL levels. It is a property of a linear maximum PN sequence that when differentially encoded, a linear operation, the resulting sequence is the same linear maximum sequence with an apparent shift in time. Thus a differential encoding scheme was not necessary with the AN/WSC-3 in differential PSK mode. The bipolar (±6v) low level teletype output of the AN/WSC-3 permitted ease of interface to the RS-232C input ("1" > 3v, "0" < 3v) of the HP-1645A Data Error Analyzer.

A strip chart recorder connected to the event output of the error analyzer provided a time history of the occurrence of the errors. From visual observation of the strip chart

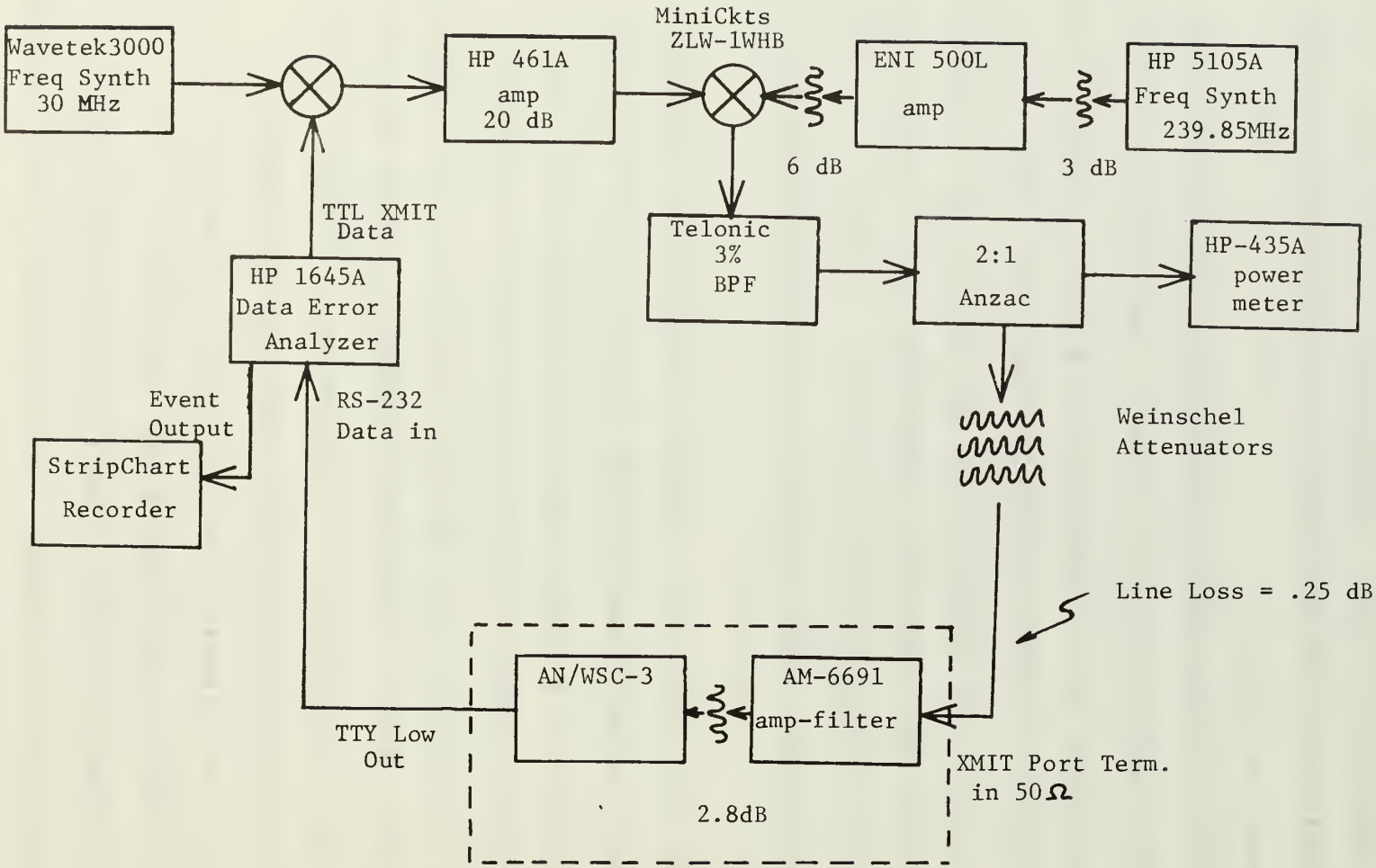

FIG. 1

Measurement Setup
Bit Error Rate

it could be determined that errors were occurring randomly, almost always in pairs, and were not bunched as a result of something unpredicted such as a line voltage transient.

The TTL level transmit sequence modulated a 30 MHz RF signal through a double balanced mixer. The 30 MHz was obtained from a Wavetek model 3000 frequency synthesizer for all testing except the 75 baud rate. The residual FM of the Wavetek synthesizer is approximately 100 Hz. This was found to affect the 75 b/s testing. For the 75 baud testing a HP-8660C frequency synthesizer was used. The residual FM of the HP-8860C is less than 10 Hz.

The 30 MHz modulated signal was amplified and heterodyned to the desired frequency selected on the receiver. All testing was accomplished at a receiver frequency of 269.850 MHz. Bit error rate was observed casually at several other receiver frequencies to insure that representative results were obtained at the chosen signal frequency. Additionally, another AN/WSC-3 was obtained on a loan basis from NAVELEX, Vallejo, and its error rate observed to comparatively insure that the AN/WSC-3 at the Naval Postgraduate School was typical. A Telonic 3% bandwidth tunable bandpass filter was utilized after the heterodyning operation to insure no undesired mixing products or oscillator spurs were transmitted to the AN/WSC-3.

The RF data signal was split for monitoring of level and the transmitted signal attenuated a desired amount by Weinschel precision calibrated attenuators. Insertion loss

through the divider and calibrated attenuators of less than 20 dB attenuation was measured directly. The loss through attenuators of greater than 20 dB attenuation was verified by comparing attenuation of equal valued attenuators on a spectrum analyzer. This permitted comparative assurance that the large valued attenuators were within manufacturer's specifications. Line loss was also accounted for. The data is therefore given for a power level at the antenna port of the AM-6691.

Figures 2 to 13 show data obtained in a format of probability of error vs. signal power for bit rates of 9600, 4800, 2400, 1200, 300, and 75 baud each for sequences with n = 20 and n = 6. All sequences are referred to by the length of the shift register generator, n. The sequence length in bits is $2^n - 1$. Testing with two sequences of different lengths was desirable for evaluation of the performance of the bit synchronizer and the effects of the periodicity of the data sequence. The slight difference in results for the two sequences is attributed to the manner in which the HP-1645A Data Error Analyzer generates the sequences by using as few shift register taps as possible. For the n = 20 sequence, 20 "1"'s are followed almost immediately by 20 "0"'s. Long unchanging data streams such as this may affect the bit synchronization loop in the receiver and thus slightly degrade performance for the n = 20 sequence. The n = 6 sequence is probably a more accurate model of typical channel data.

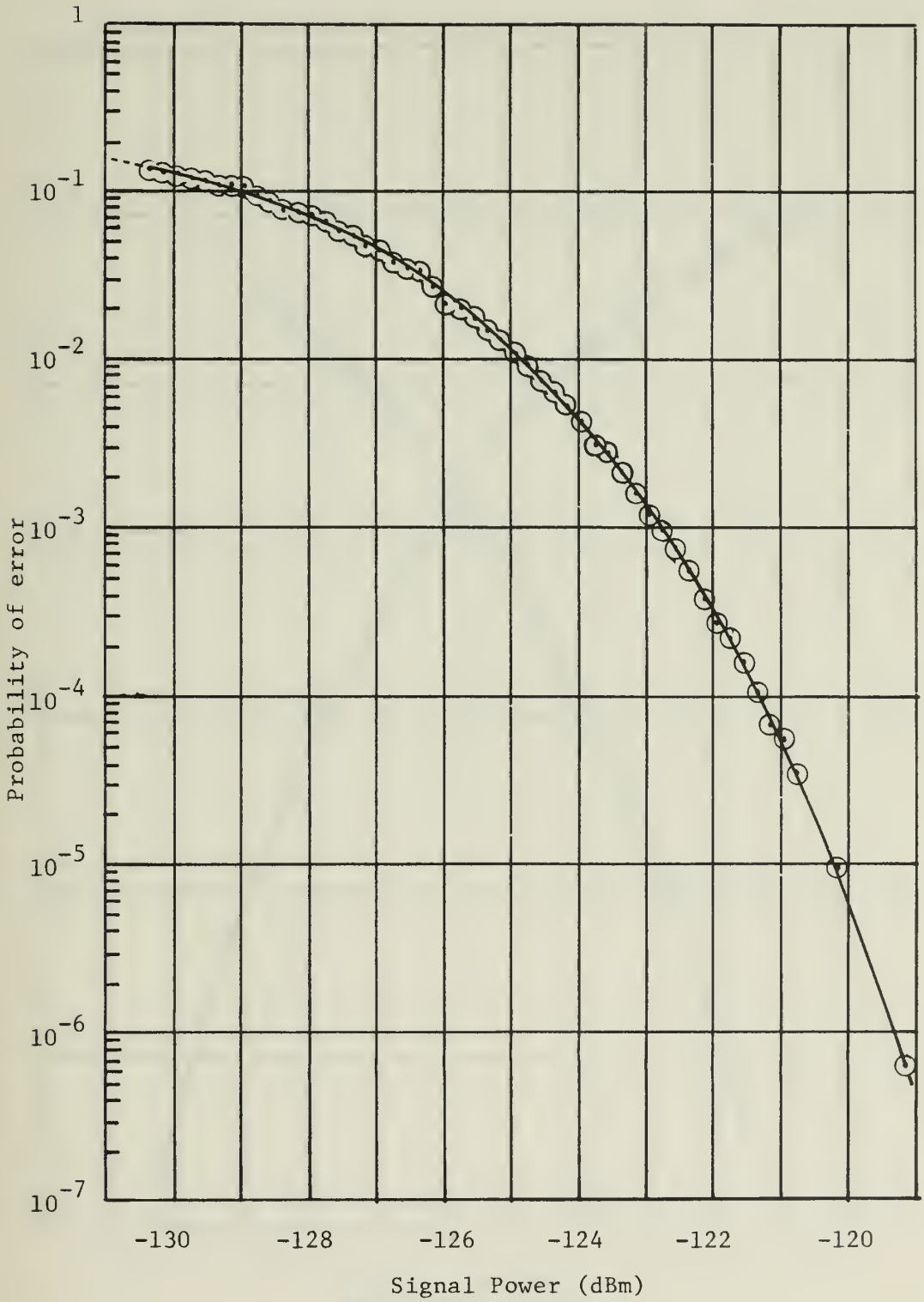

FIG. 2

AN/WSC-3 Bit Error Rate at 9600 b/s, sequence n=6

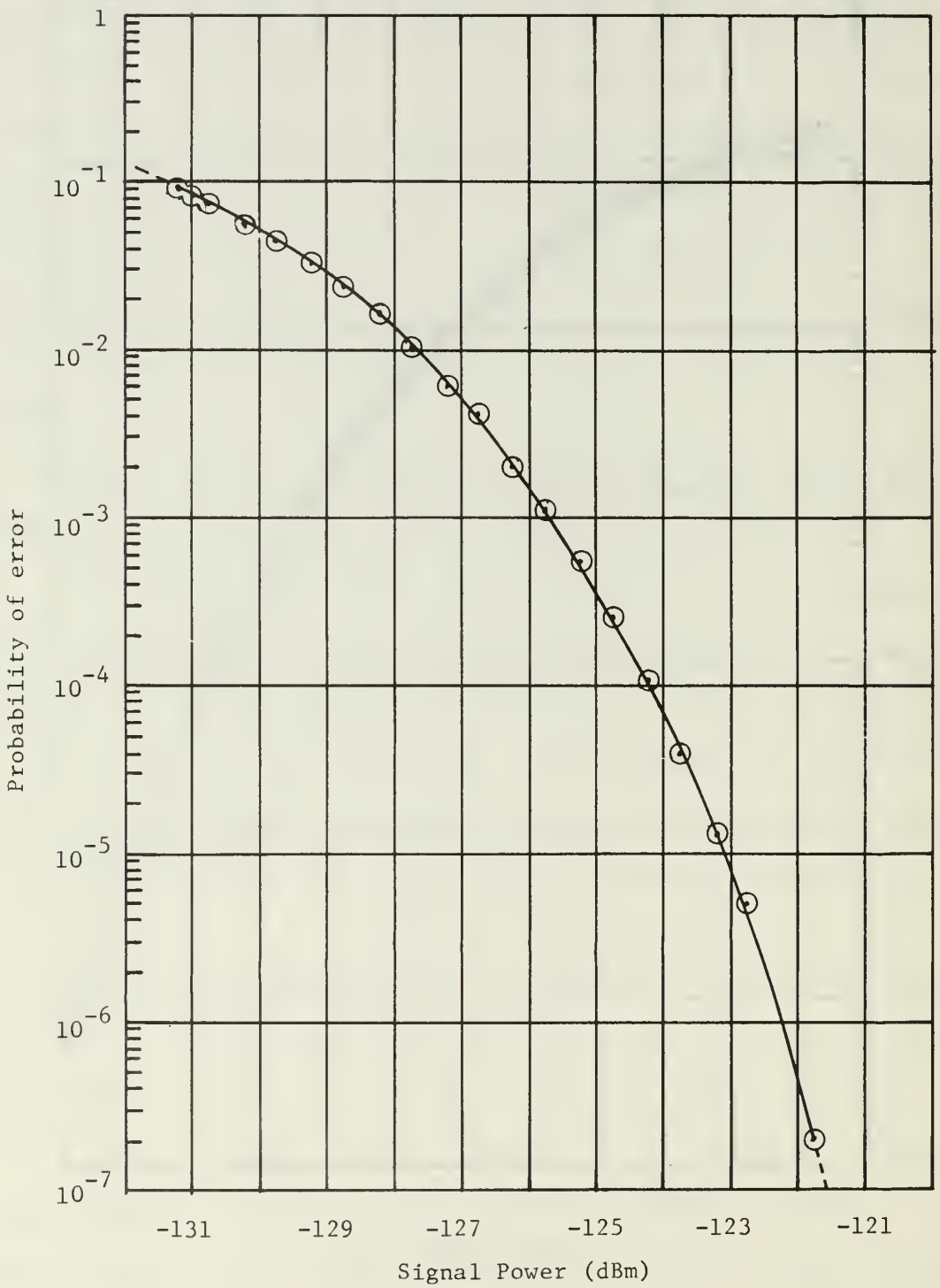

FIG. 3

AN/WSC-3 Bit Error Rate at 4800 b/s, sequence n=6

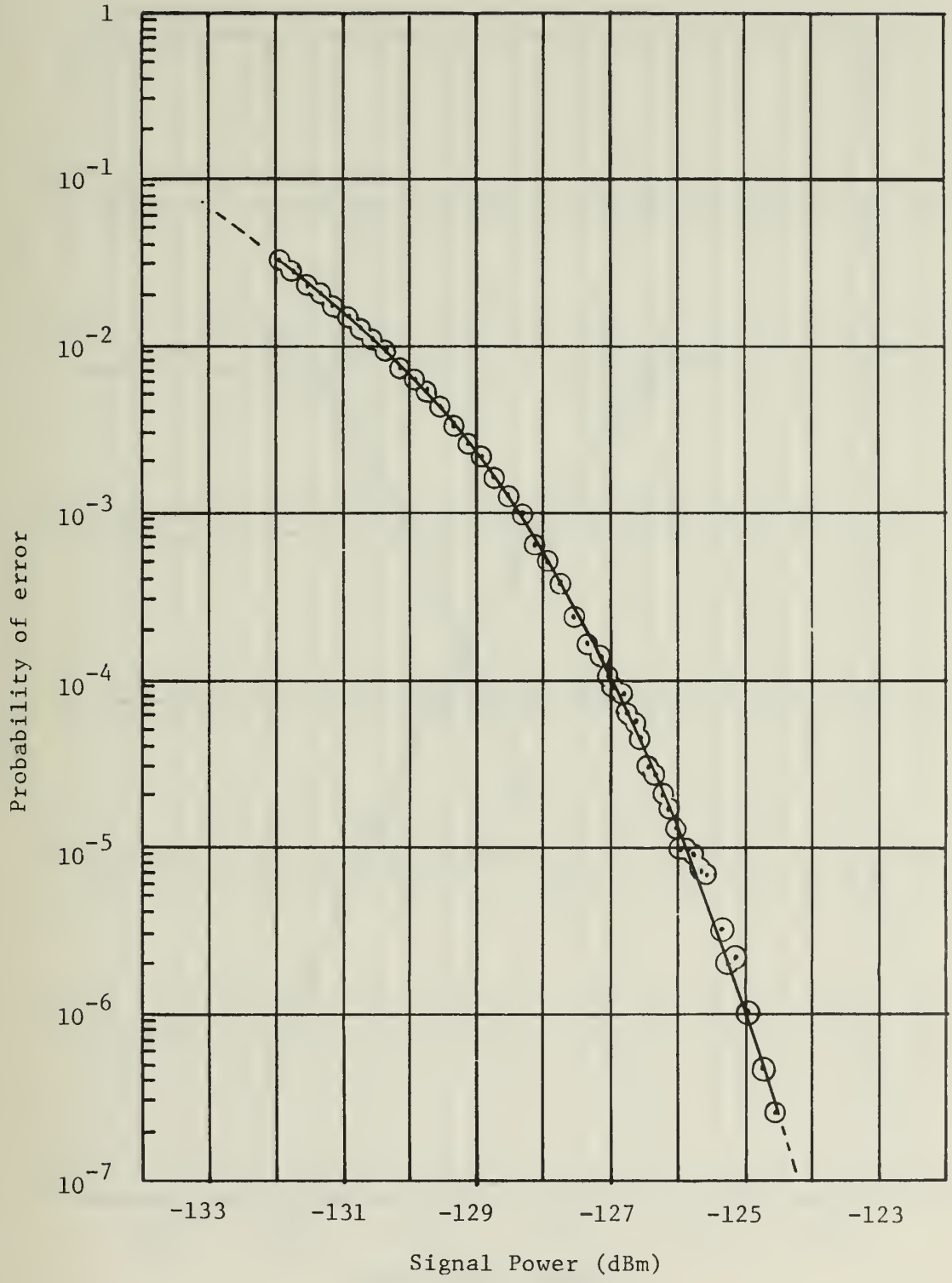

FIG. 4

AN/WSC-3 Bit Error Rate at 2400 b/s, sequence n=6

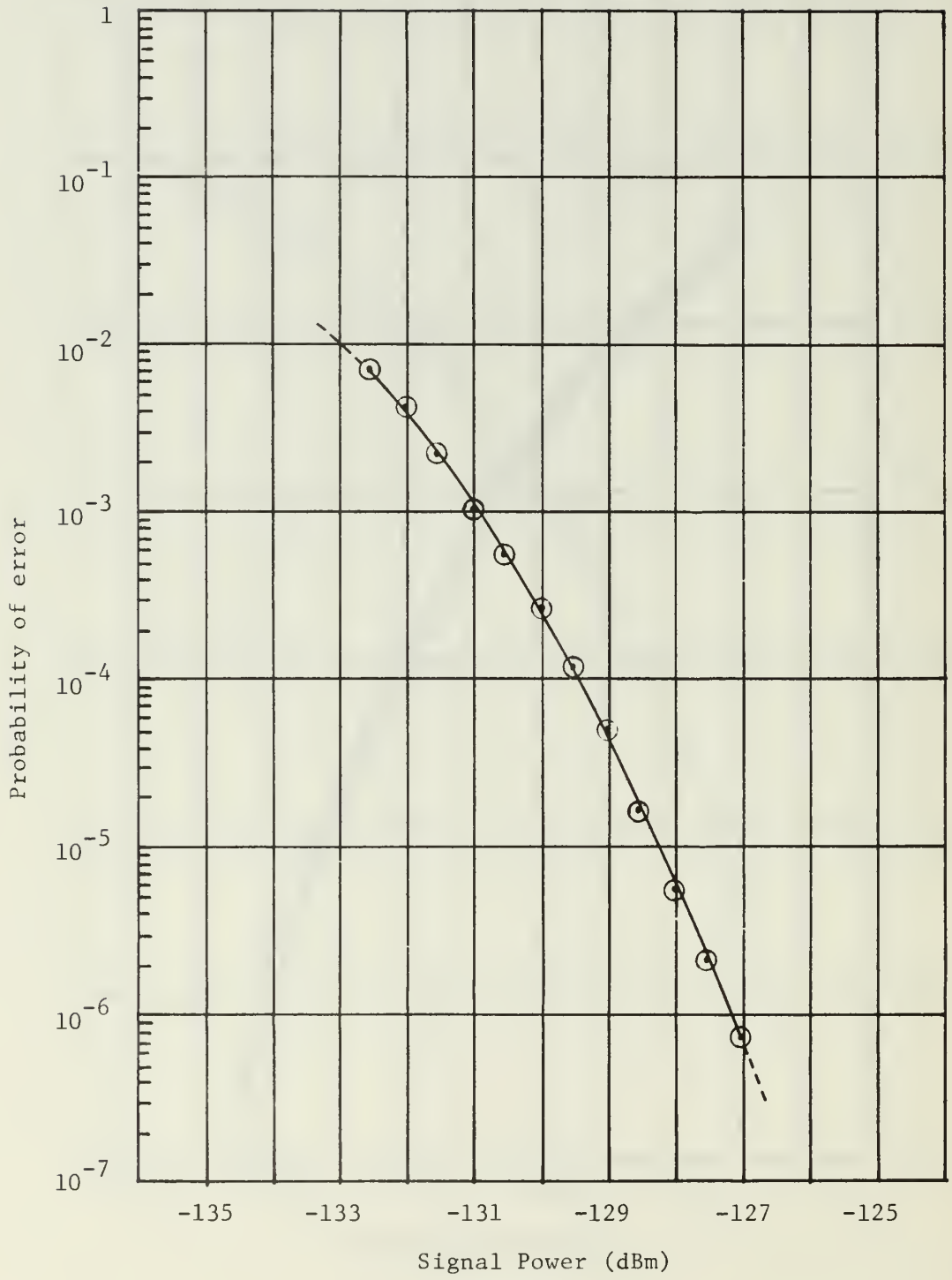

FIG. 5

AN/WSC-3 Bit Error Rate at 1200 b/s, sequence n=6

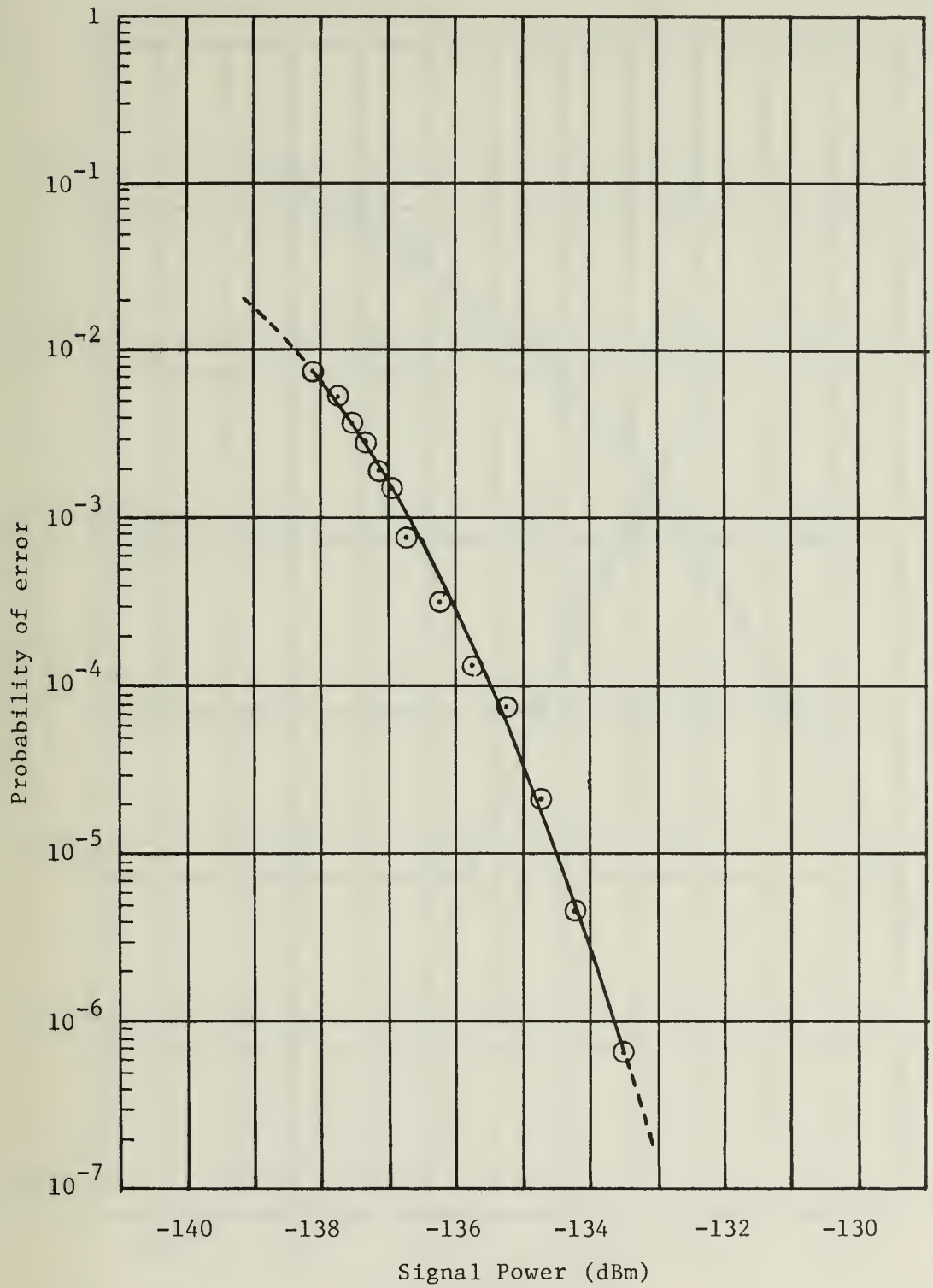

FIG. 6

AN/WSC-3 Bit Error Rate at 300 b/s, sequence n=6

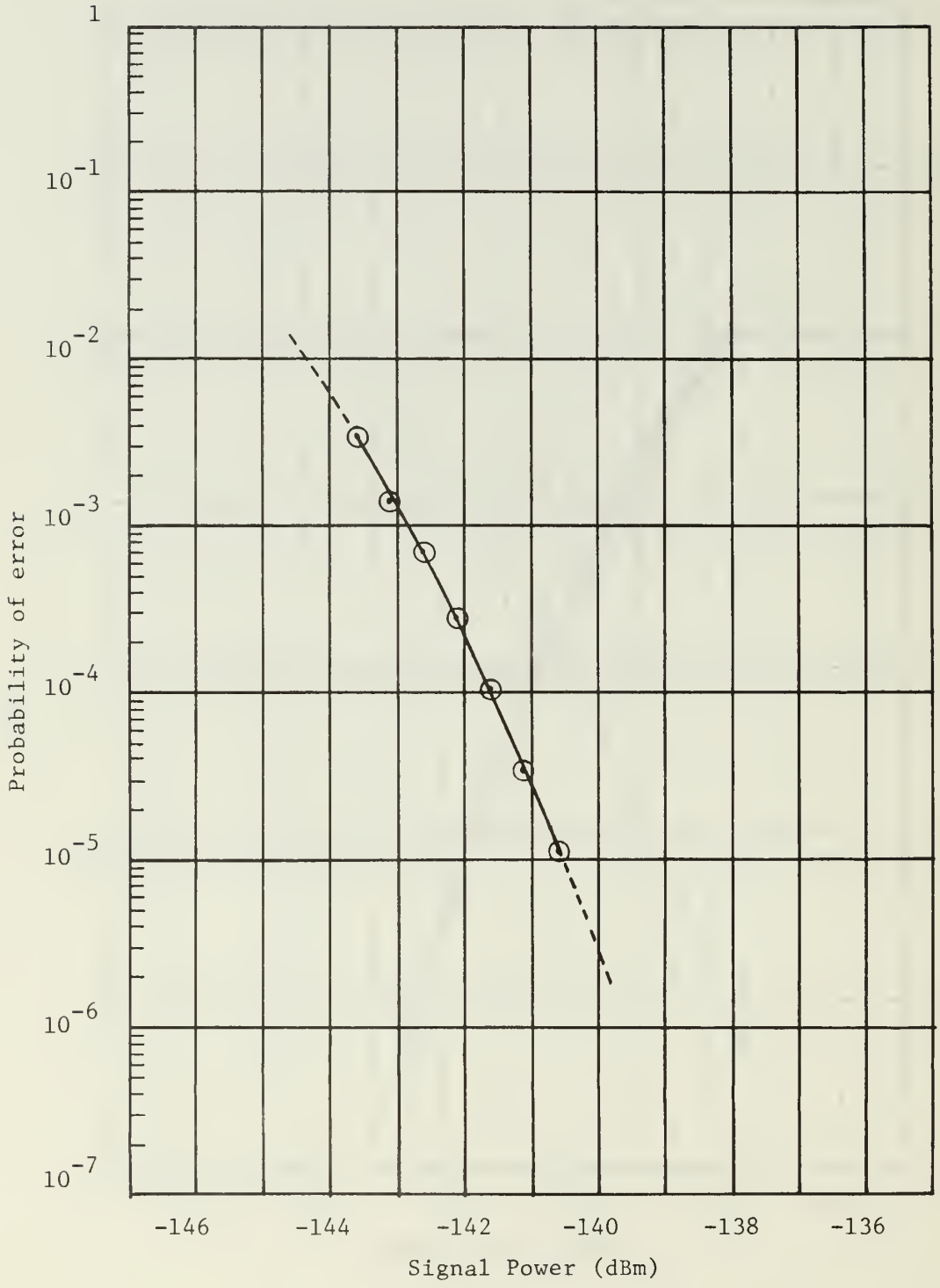

FIG. 7

AN/WSC-3 Bit Error Rate at 75 b/s, sequence n=6

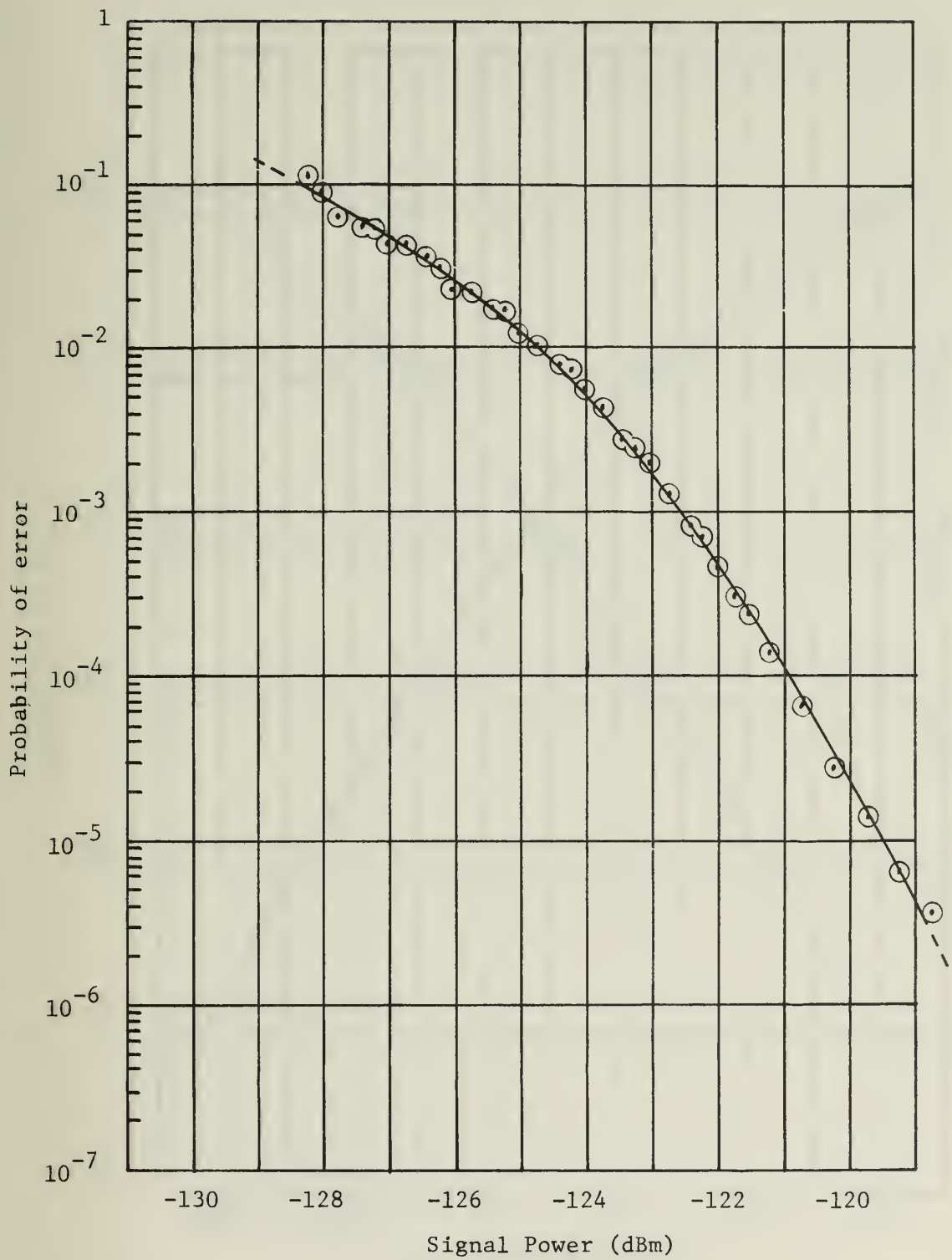

FIG. 8

AN/WSC-3 Bit Error Rate at 9600 b/s, sequence n=20

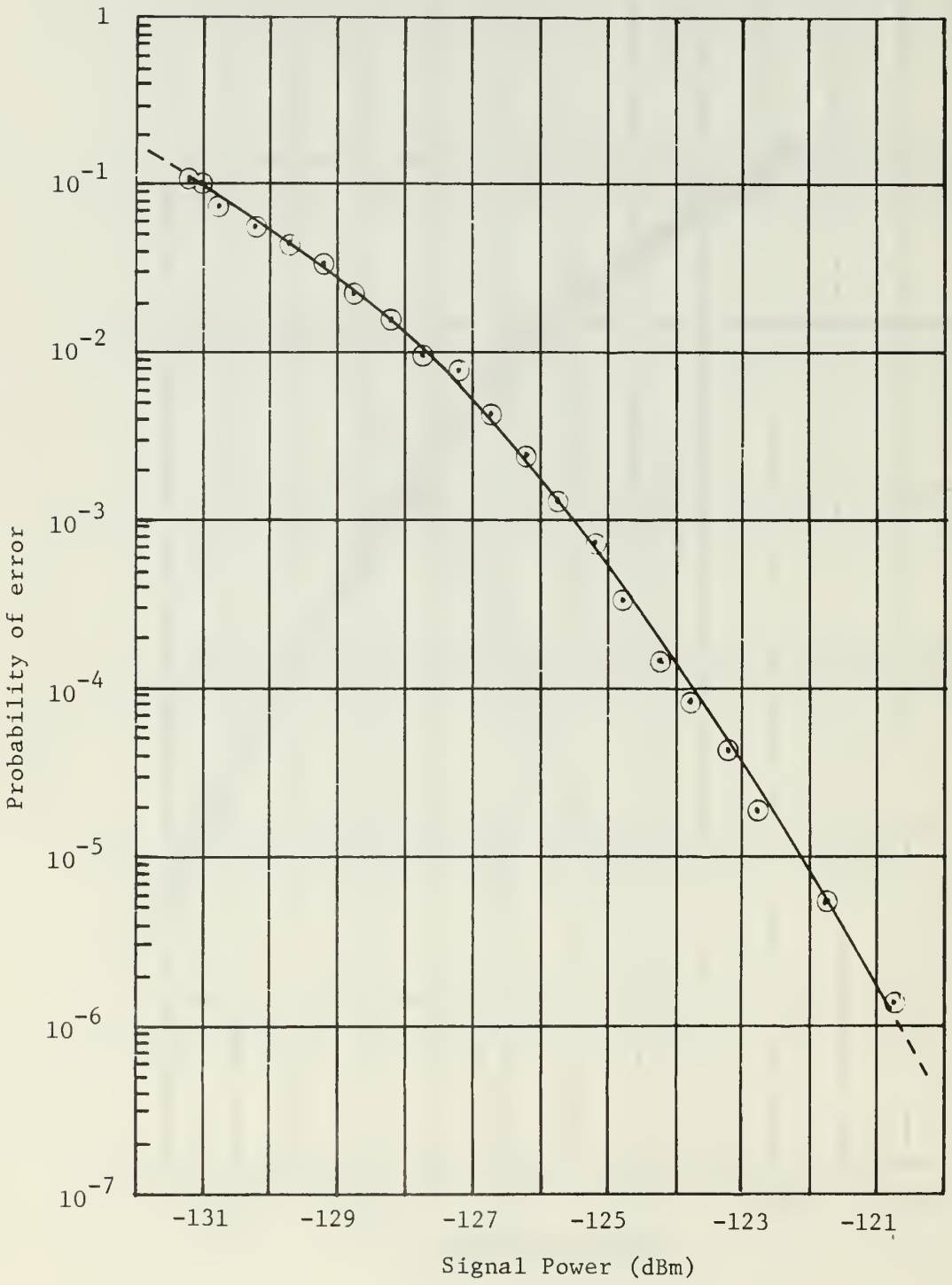

FIG. 9

AN/WSC-3 Bit Error Rate at 4800 b/s, sequence n=20

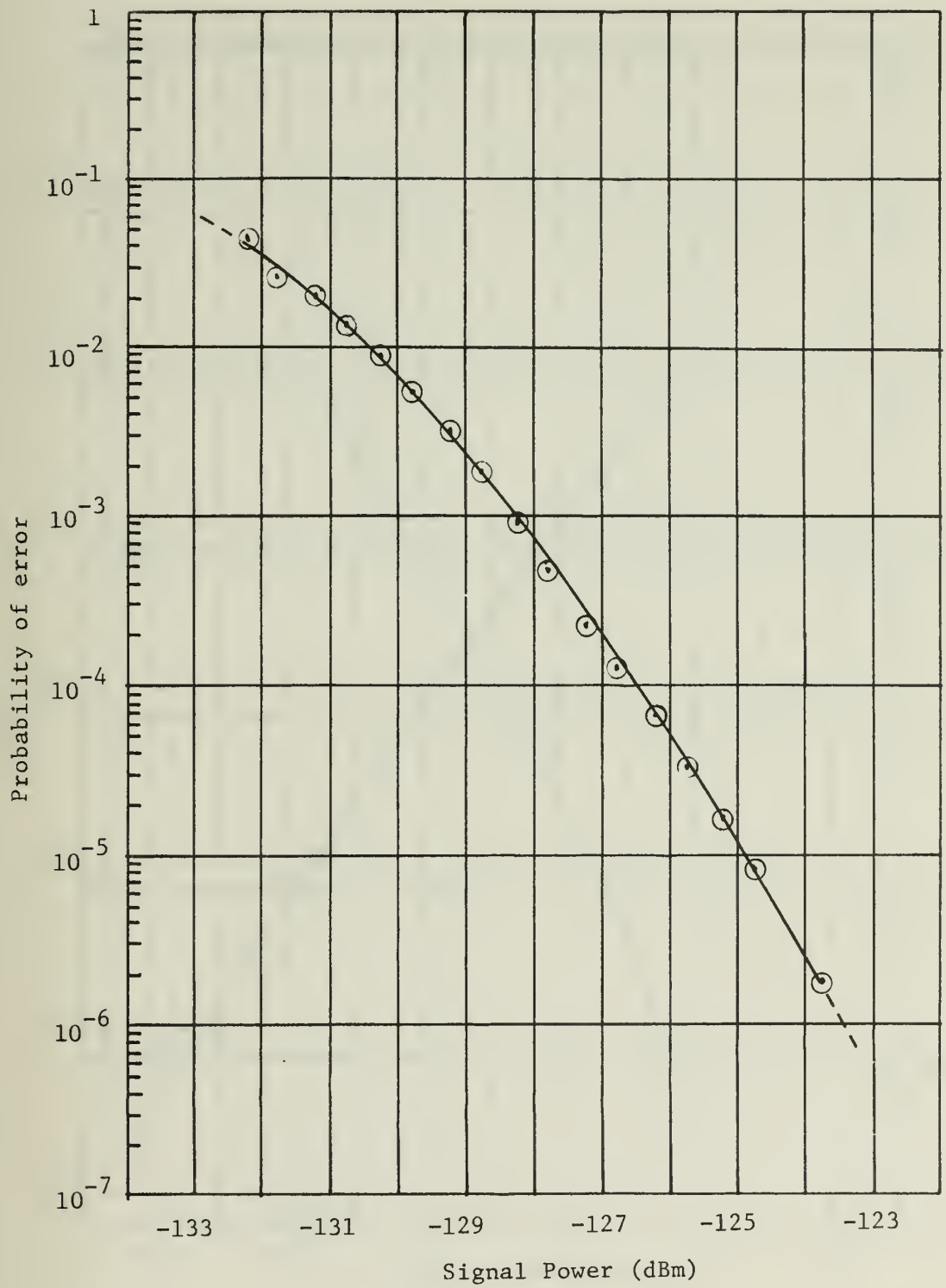

FIG. 10

AN/WSC-3 Bit Error Rate at 2400 b/s, sequence n=20

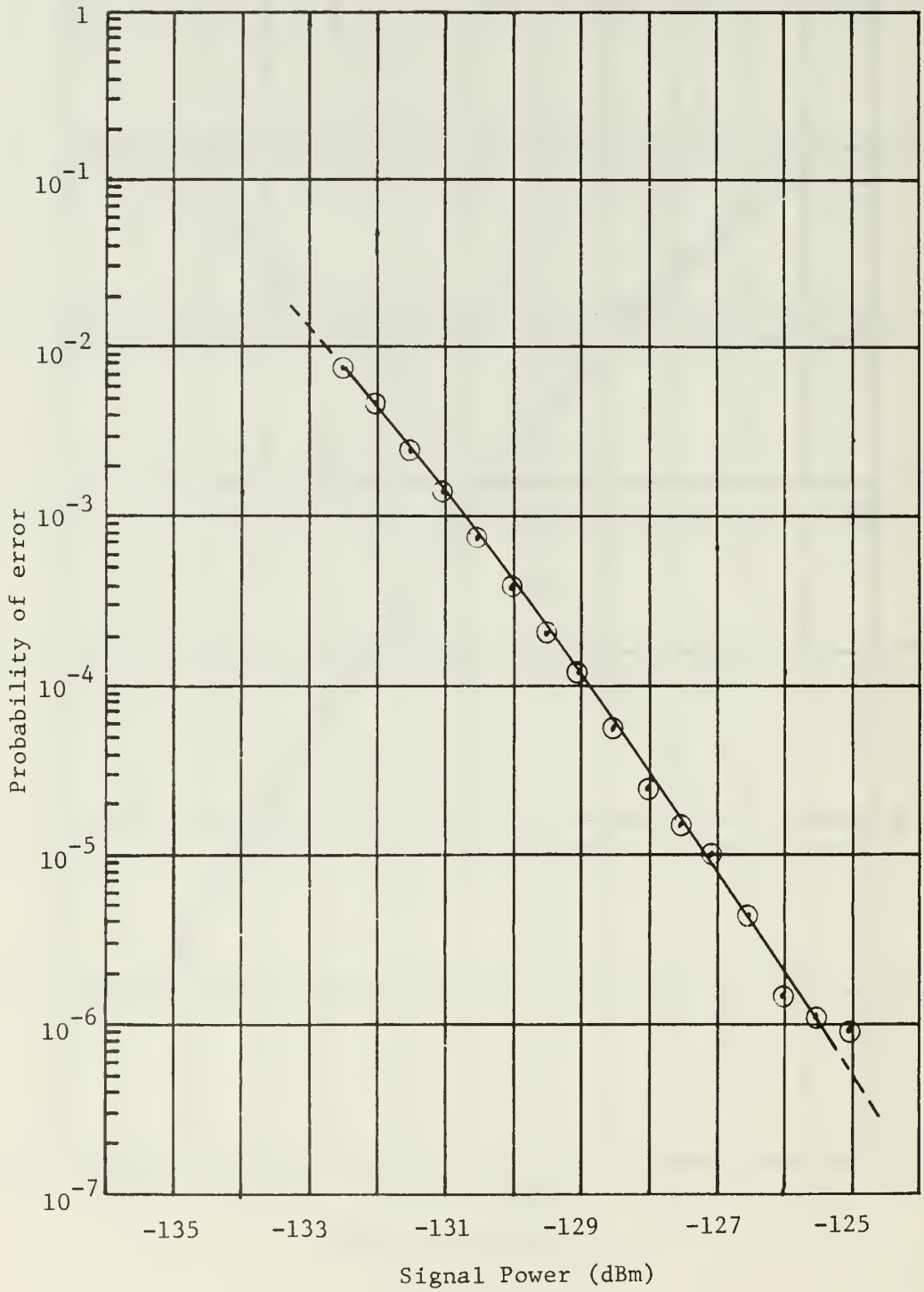

FIG. 11

AN/WSC-3 Bit Error Rate at 1200 b/s, sequence n=20

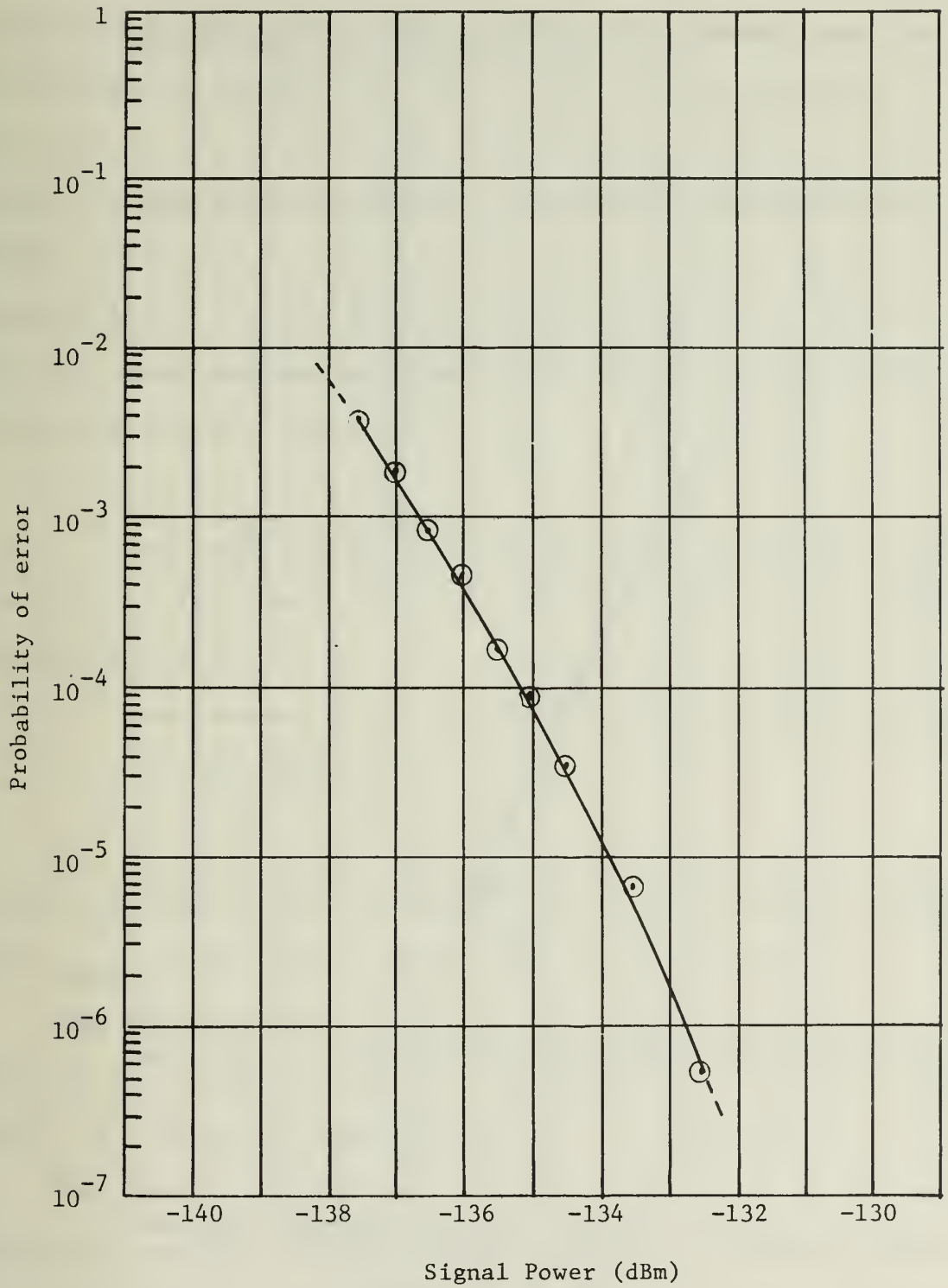

FIG. 12

AN/WSC-3 Bit error rate at 300 b/s, sequence n=20

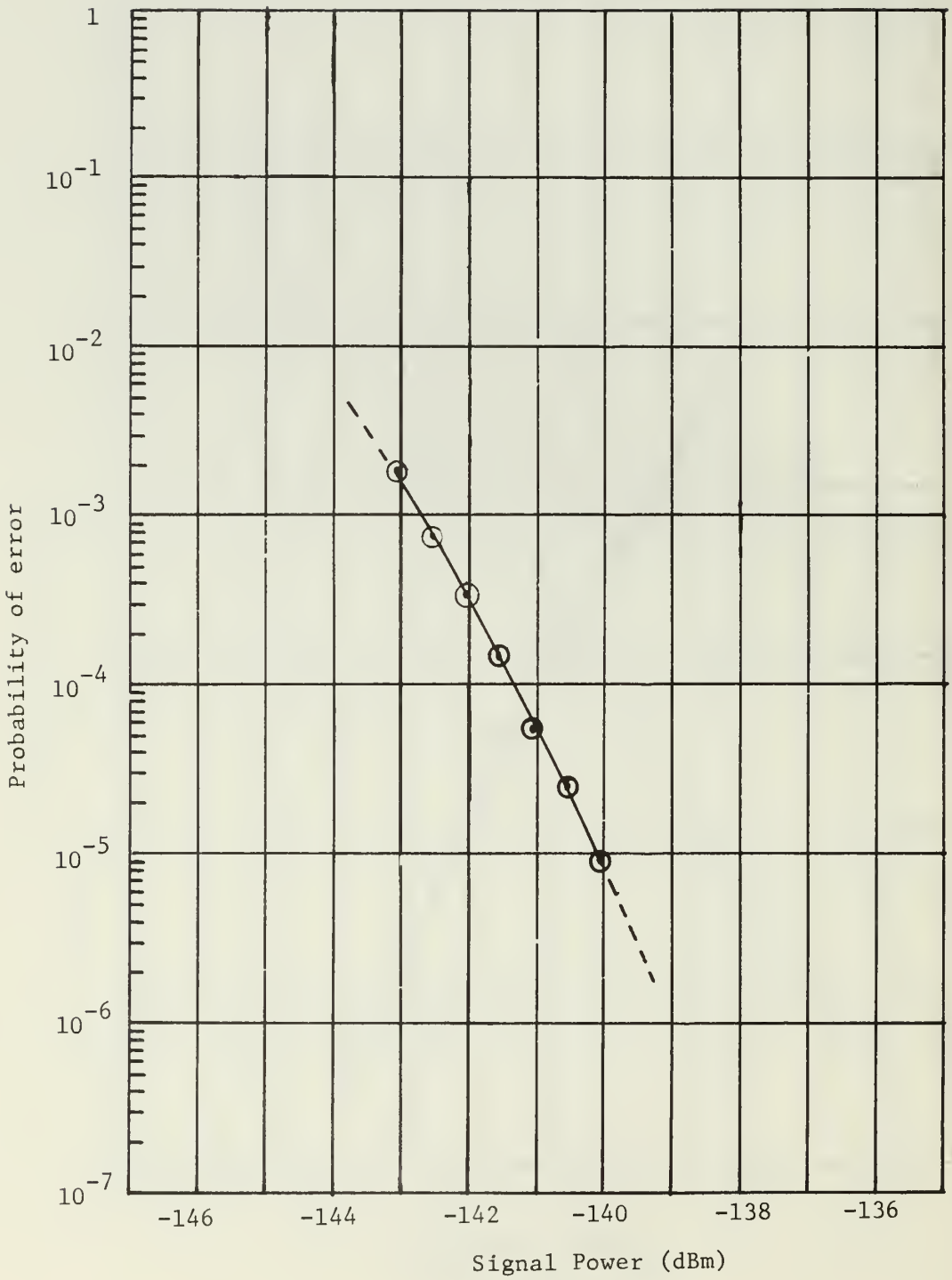

FIG. 13

AN/WSC-3 Bit Error Rate at 75 b/s, sequence n=20

In use of the signal power vs. error rate figures it must be realized that the signal generated for testing was provided by laboratory equipment with a 50 ohm source impedance. Thus the data is for a receiving system which includes an apparent antenna temperature of 290 K. A perfectly matched antenna with 50 ohm radiation resistance and no ohmic losses would of course be noiseless. Typically UHF antenna would have a noise temperature of about 100 K due to external thermal sources. Total effective antenna temperature, T_a, is given by [4].

$$T_a = T_A\eta + T_0(1 - \eta)$$

where T_A is the temperature the antenna sees, T_0 is ambient temperature and

$$\eta = \frac{R_{rad}}{R_{rad} + R_{ohmic}}$$

is the antenna efficiency and R_{rad} is the radiation resistance and R_{ohmic} is the ohmic resistance of the antenna.

The plotted data are given in Tables 1 to 12 in the Appendix along with confidence interval estimates for 95% confidence based on a gaussian approximation to the binomial distribution.

The previous comments indicate a necessity of further reducing the data to eliminate dependence on antenna temperature and provide a more useable format. The more useable format is provided by a curve of probability of error vs. E_b/N_0 a quantity which was previously defined. Determination of E_b/N_0 requires an accurate knowledge of system noise and

signal power.

There are several methods of making this calculation. First, to determine the noise temperature of the system by measurement of noise figure

$$T_s = [F-1]290 + 290 = F290$$

where T_s is the system noise temperature, F is noise figure and the additional 290 K accounts for the apparent antenna temperature of the laboratory generating system.

The system noise figure was measured using two separate recently calibrated HP-342A Noise Figure Meters and five different HP-343A VHF Noise Diodes. These measurements were then averaged to provide the data given in Figure 14. The noise figure was measured at the 70 MHz IF of the AN/WSC-3 and is referred to the antenna port of the AM-6691. The measurement was also verified by independent calculation using a solid state noise source and a spectrum analyzer.

The bit error rate data reduced to the P_e vs. E_b/N_0 format for the more typical n = 6 sequence is shown in Figure 15. Also shown for comparison is the theoretical curve and several points specified as minimum acceptable performance by original contract specifications [5].

A second technique of obtaining E_b/N_0 is to directly measure it at IF before the demodulator where it is defined. This can be accomplished with a spectrum analyzer. The energy of a baud, E_b, is easily determined from the signal power.

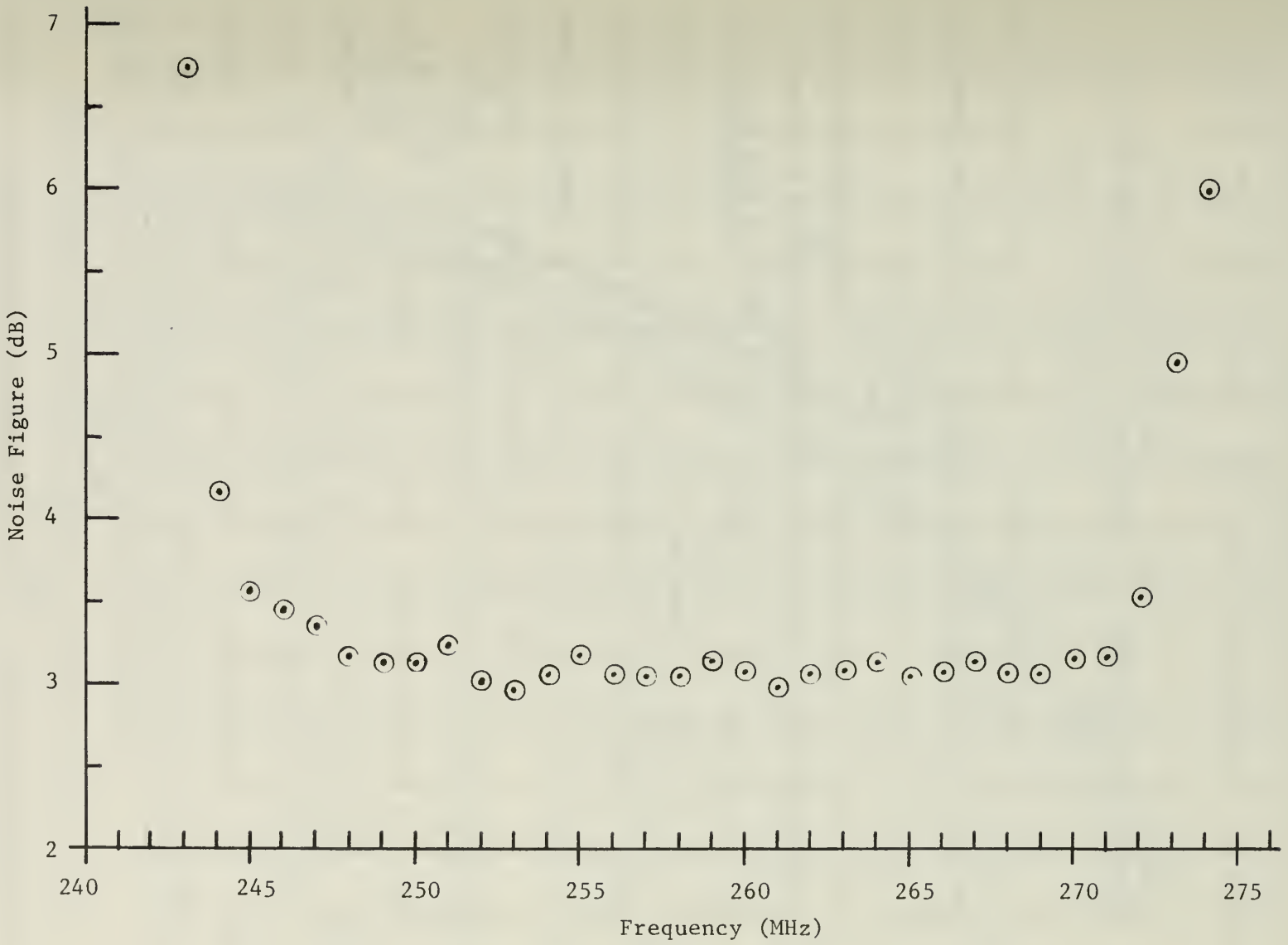

FIG. 14

AN/WSC-3 Noise Figure

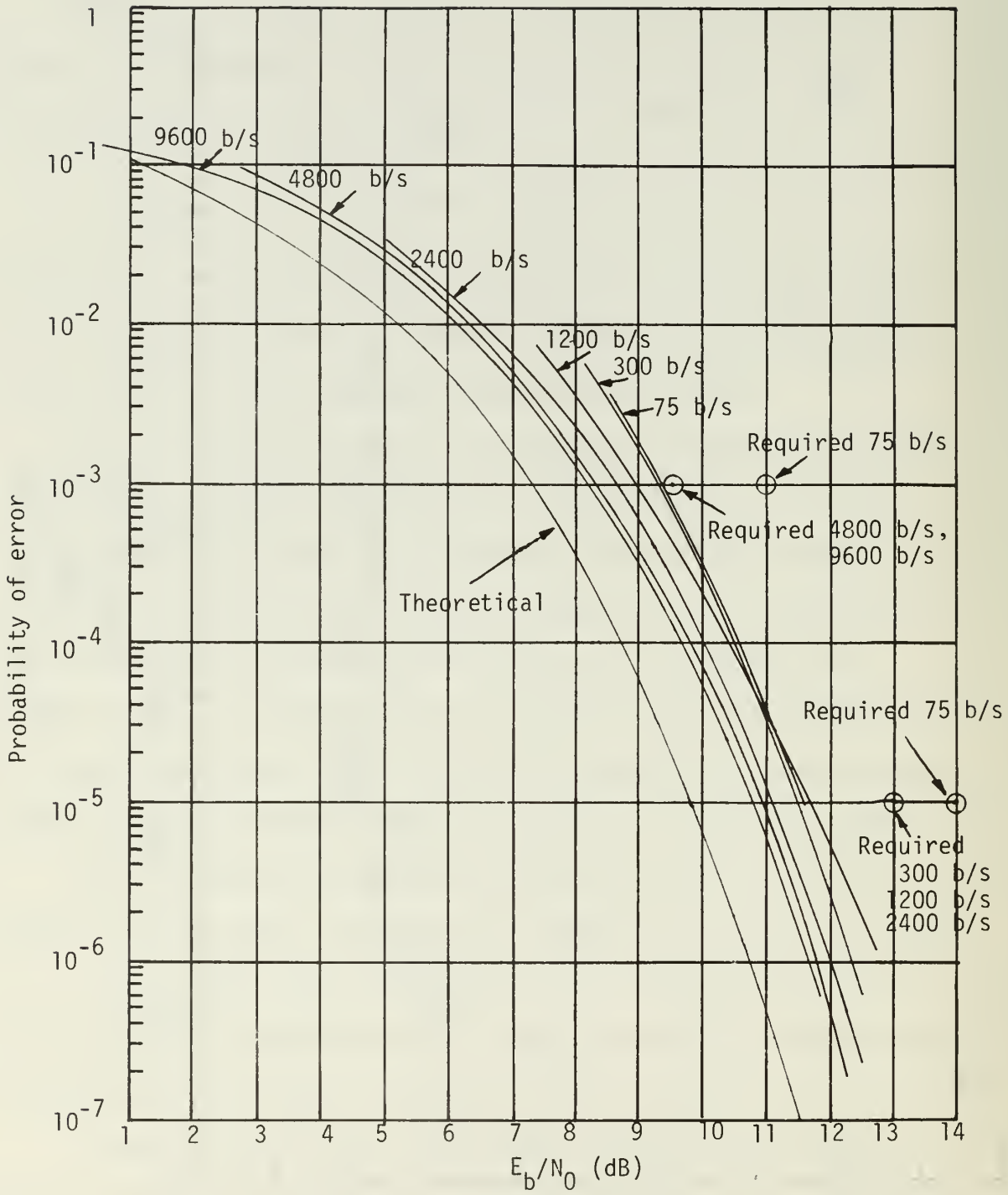

Fig. 15
Probability of Error vs. E_b/N_0 for Various Data Rates

In order to measure the noise power spectrum accurately it is necessary to consider how the spectrum analyzer operates. A simple analytical model of a spectrum analyzer is shown as

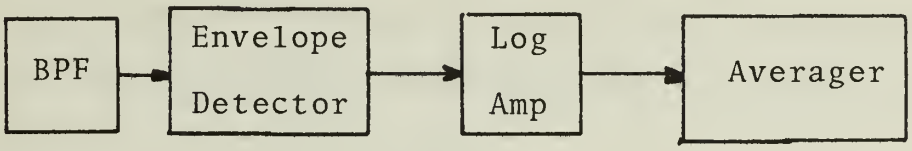

In the HP-8554B spectrum analyzer the bandpass filter is a gaussian shaped filter. The noise bandwidth of this type filter is 1.2 times the 3 dB bandwidth. Using the 10 KHz filter the accuracy of the 3 dB bandwidth is specified as ±5% by the manufacturer. Envelope detection, logging and averaging affect the distribution of the gaussian noise. Logging will amplify the noise peaks less than the rest of the noise signal so that the detected noise power appears smaller than its true value. The correction necessary to the spectrum analyzer observation is 2.5 dB [6].

This technique was used to verify the results of the method of calculating E_b/N_0 by a measurement of RF signal power. E_b/N_0 was calculated by the RF power method. Then with the setup unchanged the signal-to-noise ratio in a bandwidth equal to the data rate was observed at IF. Both of these values for E_b/N_0 were then bounded by calculated errors incurred in obtaining each measurement.

The bounded intervals for the measured E_b/N_o's were compared and found to overlap. It is therefore concluded that the worst case error bounds for E_b/N_0 in Figure 15 are ±1.0 dB.

The relative accuracy of the curves among themselves is much better. Applying the worst case errors in the measured E_b/N_o it is seen that the AN/WSC-3 is within contract specifications [5].

III. AN/SSR-1 MEASUREMENTS

Bit error rate data were obtained for the AN/SSR-1 using the experimental configuration of Figure 16. The necessity of using a different measurement configuration than for the AN/WSC-3 testing is due to the fifteen data channel and one sync channel multiplexing required of the transmitted data for the AN/SSR-1.

The installation test set performs this multiplexing operation. The sync channel, a bit by bit complement of a linear maximum sequence of length n=4, is multiplexed with data channels containing "The quick brown fox...." at a 1200 bit per second rate. Errors in the output of the sync channel at a 75 baud rate are counted on a bit error rate monitor "BERM" obtained as a prototype from Motorola, Inc. A deficiency of the BERM is that its maximum preset counter is 10^6 bits. Thus only error rates worse than 1×10^{-6} can reliably be measured.

Noise figure of the AN/SSR-1 was measured and found to be 2.5 dB measured at the 20 MHz IF into the vector combiner and referenced to the antenna port of the amplifier downconverter. The measurement was made with a precision solid state noise source and a spectrum analyzer using the "Y-factor" method as the 20 MHz IF could not be accommodated on the HP-342A noise figure meter.

Figure 17 shows the data obtained as a function of signal power. Data were taken for two conditions of the combiner, first with data applied to only one channel of the

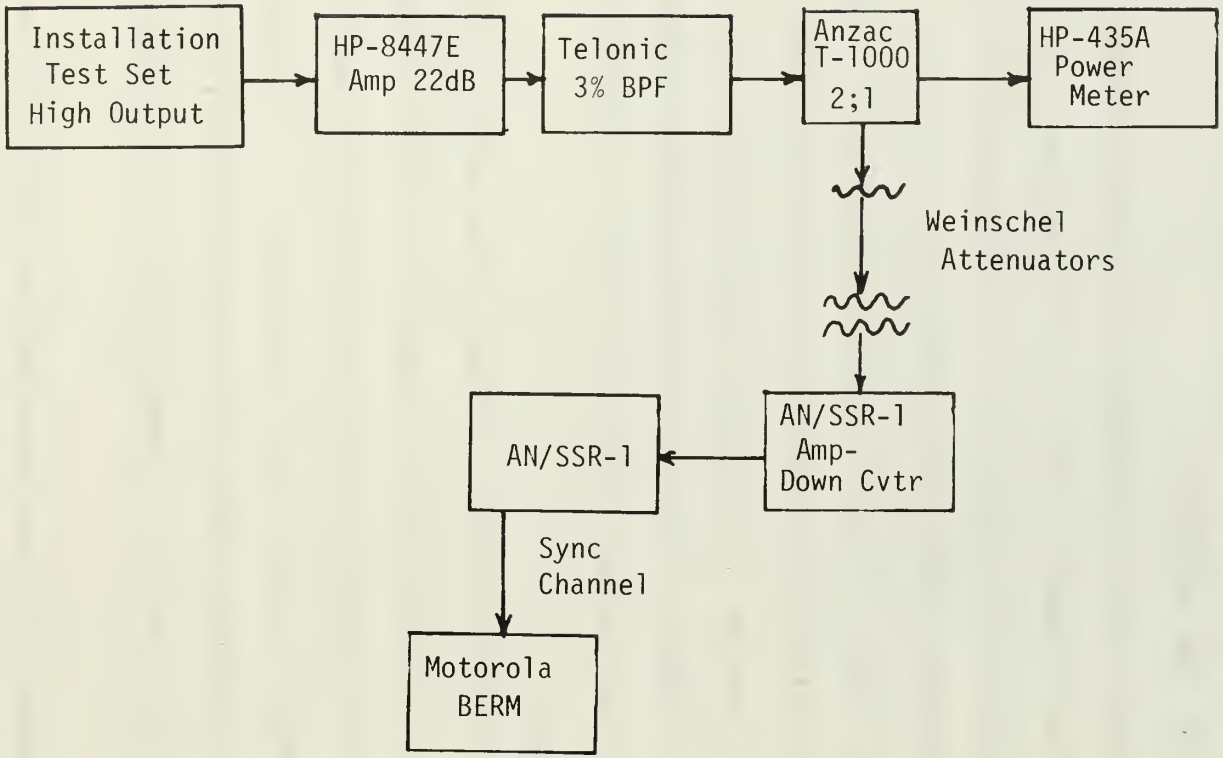

Fig. 16

Experiment Configuration

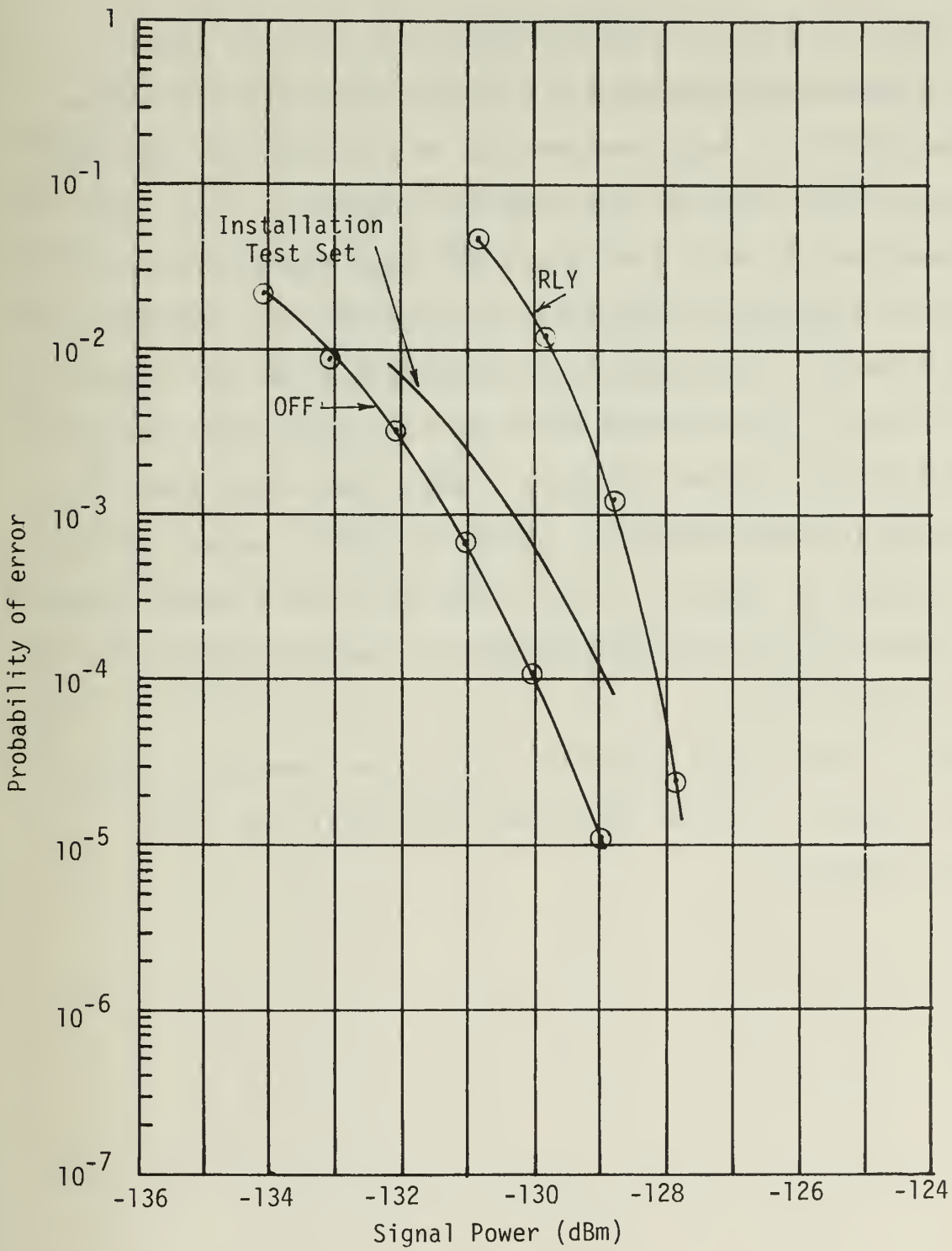

Fig. 17

AN/SSR-1 Bit Error Rate

combiner and the other channels terminated in their characteristic impedances, referred to as the "RLY"position; second, with data applied to only one channel of the combiner and the other channels not used in the combiner, referred to as the "OFF" position. As expected, the additional thermal noise applied to the combiner by having the channels resistively terminated causes a degradation of performance at low signal-to-noise ratios. It is noted that the two curves are coming together at higher signal-to-noise ratios indicating that the vector combiner works better at higher signal-to-noise ratios.

Also shown in Figure 17 is a bit error rate curve taken from the installation test set manual [7] and reproduced for comparative purposes.

Tables 13 and 14 in Appendix 1 give the numerical values plotted in Figure 17 and confidence intervals for a .95 confidence interval.

IV. CONCLUSIONS

The performance of the AN/SSR-1 and AN/WSC-3 satellite communications receivers with random uncoded data has been reported. This performance characterization has been accomplished by measurement of Bit Error Rate. An expression for the theoretical performance of the AN/WSC-3 has been developed. The receiver's noise figure has been reported. Confidence limits have been developed to bound the measured data.

The data for the AN/WSC-3 has been reduced to the format of probability of error vs. E_b/N_0. In comparison of this data to contract specifications [5] it is seen that the worst case error bound of the measurements is within the specified performance.

APPENDIX A

TABLE 1

BIT ERROR RATE MEASUREMENTS

Data Rate = 9600 b/s

Sequence Length = 2^6-1

P_{Signal}	$\hat{p}$	c	$U_{.95}$	$L_{.95}$
-130.35	1.429×10^{-1}	1429	1.534×10^{-1}	1.324×10^{-1}
-130.15	1.336×10^{-1}	4007	1.395×10^{-1}	1.277×10^{-1}
-129.95	1.299×10^{-1}	3897	1.357×10^{-1}	1.241×10^{-1}
-129.75	1.253×10^{-1}	3760	1.310×10^{-1}	1.196×10^{-1}
-129.55	1.192×10^{-1}	3575	1.247×10^{-1}	1.137×10^{-1}
-129.35	1.081×10^{-1}	3244	1.134×10^{-1}	1.028×10^{-1}
-129.15	1.080×10^{-1}	3241	1.133×10^{-1}	1.027×10^{-1}
-128.95	1.014×10^{-1}	3043	1.065×10^{-1}	9.630×10^{-2}
-128.75	9.270×10^{-2}	2781	9.757×10^{-2}	8.783×10^{-2}
-128.55	8.857×10^{-2}	2657	9.333×10^{-2}	8.381×10^{-2}
-128.35	7.973×10^{-2}	2392	8.425×10^{-2}	7.521×10^{-2}
-128.15	7.457×10^{-2}	2237	7.894×10^{-2}	7.020×10^{-2}
-127.95	7.123×10^{-2}	2137	7.550×10^{-2}	6.696×10^{-2}
-127.75	6.827×10^{-2}	2048	7.245×10^{-2}	6.409×10^{-2}
-127.55	5.840×10^{-2}	1752	6.227×10^{-2}	5.453×10^{-2}
-127.35	5.357×10^{-2}	1607	5.726×10^{-2}	4.987×10^{-2}
-127.15	4.787×10^{-2}	1436	5.137×10^{-2}	4.437×10^{-2}
-126.95	4.314×10^{-2}	2157	4.571×10^{-2}	4.057×10^{-2}
-126.75	3.870×10^{-2}	1161	4.185×10^{-2}	3.555×10^{-2}
-126.55	3.473×10^{-2}	1042	3.771×10^{-2}	3.175×10^{-2}
-126.35	3.413×10^{-2}	1024	3.709×10^{-2}	3.117×10^{-2}
-126.15	2.660×10^{-2}	798	2.921×10^{-2}	2.399×10^{-2}
-125.95	2.150×10^{-2}	645	2.385×10^{-2}	1.915×10^{-2}
-125.75	2.063×10^{-2}	6188	2.136×10^{-2}	1.990×10^{-2}
-125.55	1.808×10^{-2}	5423	1.876×10^{-2}	1.740×10^{-2}
-125.35	1.558×10^{-2}	4675	1.621×10^{-2}	1.495×10^{-2}
-125.15	1.378×10^{-2}	4133	1.437×10^{-2}	1.319×10^{-2}
-124.95	1.096×10^{-2}	3288	1.149×10^{-2}	1.043×10^{-2}
-124.75	9.367×10^{-3}	2810	9.857×10^{-3}	8.877×10^{-3}
-124.55	7.687×10^{-3}	2306	8.131×10^{-3}	7.243×10^{-3}

-124.35	6.330×10^{-3}	1899	6.733×10^{-3}	5.927×10^{-3}
-124.15	5.217×10^{-3}	1565	5.583×10^{-3}	4.851×10^{-3}
-123.95	4.327×10^{-3}	1298	4.660×10^{-3}	3.994×10^{-3}
-123.75	3.227×10^{-3}	968	3.514×10^{-3}	2.940×10^{-3}
-123.55	2.863×10^{-3}	859	3.134×10^{-3}	2.592×10^{-3}
-123.35	2.208×10^{-3}	6625	2.283×10^{-3}	2.133×10^{-3}
-123.15	1.707×10^{-3}	6826	1.764×10^{-3}	1.650×10^{-3}
-122.95	1.268×10^{-3}	7605	1.308×10^{-3}	1.228×10^{-3}
-122.75	9.727×10^{-4}	6809	1.005×10^{-3}	9.400×10^{-4}
-122.55	7.617×10^{-4}	2285	8.059×10^{-4}	7.175×10^{-4}
-122.35	5.577×10^{-4}	1673	5.955×10^{-4}	5.199×10^{-4}
-122.15	3.891×10^{-4}	1559	4.164×10^{-4}	3.816×10^{-4}
-121.95	2.943×10^{-4}	883	3.218×10^{-4}	2.668×10^{-4}
-121.75	2.230×10^{-4}	669	2.469×10^{-4}	1.991×10^{-4}
-121.55	1.713×10^{-4}	514	1.922×10^{-4}	1.504×10^{-4}
-121.35	1.055×10^{-4}	2109	1.119×10^{-4}	9.913×10^{-5}
-121.15	6.997×10^{-5}	2099	7.420×10^{-5}	6.574×10^{-5}
-120.95	5.780×10^{-5}	1156	6.251×10^{-5}	5.309×10^{-5}
-120.75	3.540×10^{-5}	354	4.062×10^{-5}	3.018×10^{-5}
-120.15	9.740×10^{-6}	974	1.061×10^{-5}	8.875×10^{-6}
-119.15	6.306×10^{-7}	231	7.456×10^{-7}	5.156×10^{-7}

TABLE 2

BIT ERROR RATE MEASUREMENTS

Data Rate = 4800 b/s

Sequence Length = 2^6-1

P_{Signal}	$\hat{p}$	c	$U_{.95}$	$L_{.95}$
-131.25	9.065×10^{-2}	5439	9.406×10^{-2}	8.724×10^{-2}
-131.05	8.357×10^{-2}	5014	8.684×10^{-2}	8.030×10^{-2}
-130.75	7.288×10^{-2}	4373	7.593×10^{-2}	6.983×10^{-2}
-130.25	5.827×10^{-2}	3496	6.100×10^{-2}	5.554×10^{-2}
-129.75	4.517×10^{-2}	2710	4.758×10^{-2}	4.276×10^{-2}
-129.25	3.228×10^{-2}	1937	3.431×10^{-2}	3.025×10^{-2}
-128.75	2.150×10^{-2}	1290	2.316×10^{-2}	1.984×10^{2}
-128.25	1.670×10^{-2}	1002	1.816×10^{-2}	1.524×10^{-2}
-127.75	1.082×10^{-2}	649	1.200×10^{-2}	9.643×10^{-3}
-127.25	6.133×10^{-3}	368	7.019×10^{-3}	5.247×10^{-3}
-126.75	4.033×10^{-3}	2420	4.260×10^{-3}	3.806×10^{-3}
-126.25	2.002×10^{-3}	1201	2.162×10^{-3}	1.842×10^{-3}
-125.75	1.160×10^{-3}	696	1.282×10^{-3}	1.038×10^{-3}
-125.25	5.483×10^{-4}	329	6.321×10^{-4}	4.645×10^{-4}
-124.75	2.603×10^{-4}	781	2.861×10^{-4}	2.345×10^{-4}
-124.25	1.107×10^{-4}	332	1.275×10^{-4}	9.386×10^{-5}
-123.75	4.067×10^{-5}	122	5.088×10^{-5}	3.046×10^{-5}
-123.25	1.375×10^{-5}	275	1.605×10^{-5}	1.145×10^{-5}
-122.75	5.000×10^{-6}	100	6.386×10^{-6}	3.614×10^{-6}
-121.75	2.000×10^{-7}	20	3.240×10^{-7}	7.604×10^{-8}

TABLE 3

BIT ERROR RATE MEASUREMENTS

Data Rate = 2400 b/s

Sequence Length = 2^6-1

P_{Signal}	$\hat{p}$	c	$U_{.95}$	$L_{.95}$
-131.95	3.301×10^{-2}	2971	3.469×10^{-2}	3.133×10^{-2}
-131.75	2.807×10^{-2}	1684	2.997×10^{-2}	2.617×10^{-2}
-131.55	2.403×10^{-2}	1442	2.578×10^{-2}	2.228×10^{-2}
-131.35	2.095×10^{-2}	1257	2.259×10^{-2}	1.931×10^{-2}
-131.15	1.818×10^{-2}	10905	1.866×10^{-2}	1.770×10^{-2}
-130.95	1.589×10^{-2}	9536	1.634×10^{-2}	1.544×10^{-2}
-130.75	1.344×10^{-2}	8064	1.385×10^{-2}	1.303×10^{-2}
-130,55	1.113×10^{-2}	6676	1.151×10^{-2}	1.075×10^{-2}
-130.35	9.533×10^{-3}	5720	9.882×10^{-3}	9.184×10^{-3}
-130.15	7.480×10^{-3}	4488	7.789×10^{-3}	7.171×10^{-3}
-129.95	6.428×10^{-3}	3857	6.715×10^{-3}	6.141×10^{-3}
-129.75	5.407×10^{-3}	3244	5.670×10^{-3}	5.144×10^{-3}
-129.55	4.293×10^{-3}	2576	4.527×10^{-3}	4.059×10^{-3}
-129.35	3.397×10^{-3}	2038	3.606×10^{-3}	3.188×10^{-3}
-129.15	2.708×10^{-3}	1625	2.894×10^{-3}	2.522×10^{-3}
-128.95	2.228×10^{-3}	1337	2.397×10^{-3}	2.059×10^{-3}
-128.75	1.711×10^{-3}	6843	1.768×10^{-3}	1.654×10^{-3}
-128.55	1.337×10^{-3}	5347	1.388×10^{-3}	1.286×10^{-3}
-128.35	1.004×10^{-3}	4017	1.048×10^{-3}	9.601×10^{-4}
-128.15	6.623×10^{-4}	2649	6.980×10^{-4}	6.266×10^{-4}
-127.95	5.093×10^{-4}	2037	5.406×10^{-4}	4.780×10^{-4}
-127.75	3.953×10^{-4}	1581	4.229×10^{-4}	3.677×10^{-4}
-127.55	2.748×10^{-4}	1099	2.978×10^{-4}	2.518×10^{-4}
-127.35	1.863×10^{-4}	745	2.052×10^{-4}	1.674×10^{-4}
-127.15	1.455×10^{-4}	582	1.622×10^{-4}	1.288×10^{-4}
-127.05	1.073×10^{-4}	1073	1.164×10^{-4}	9.822×10^{-5}
-126.95	9.060×10^{-5}	906	9.894×10^{-5}	8.226×10^{-5}
-126.85	8.220×10^{-5}	822	9.015×10^{-5}	7.425×10^{-5}
-126.75	6.580×10^{-5}	658	7.291×10^{-5}	5.869×10^{-5}

-126.65	5.890×10^{-5}	589	6.563×10^{-5}	5.217×10^{-5}
-126.55	4.490×10^{-5}	449	5.077×10^{-5}	3.903×10^{-5}
-126.45	3.060×10^{-5}	306	3.545×10^{-5}	2.575×10^{-5}
-126.35	2.750×10^{-5}	275	3.210×10^{-5}	2.290×10^{-5}
-126.25	2.040×10^{-5}	204	2.436×10^{-5}	1.644×10^{-5}
-126.15	1.750×10^{-5}	175	2.117×10^{-5}	1.383×10^{-5}
-126.05	1.370×10^{-5}	137	1.694×10^{-5}	1.046×10^{-5}
-125.95	9.800×10^{-6}	98	1.254×10^{-5}	7.056×10^{-6}
-125.85	9.500×10^{-6}	95	1.220×10^{-5}	6.798×10^{-6}
-125.75	9.000×10^{-6}	90	1.163×10^{-5}	6.370×10^{-6}
-125.65	7.200×10^{-6}	72	9.552×10^{-6}	4.848×10^{-6}
-125.55	7.000×10^{-6}	70	9.319×10^{-6}	4.681×10^{-6}
-125.35	2.300×10^{-6}	23	3.629×10^{-6}	9.707×10^{-7}
-125.25	2.030×10^{-6}	203	2.425×10^{-6}	1.635×10^{-6}
-125.15	2.270×10^{-6}	227	2.688×10^{-6}	1.852×10^{-6}
-124.95	1.010×10^{-6}	101	1.289×10^{-6}	7.314×10^{-7}
-124.75	4.800×10^{-7}	48	6.720×10^{-6}	2.880×10^{-7}
-124.55	2.656×10^{-7}	93	3.419×10^{-7}	1.893×10^{-7}

TABLE 4

BIT ERROR RATE MEASUREMENTS

Data Rate = 1200 b/s

Sequence Length = 2^6-1

P_{Signal}	$\hat{p}$	c	$U_{.95}$	$L_{.95}$
-132.53	7.107×10^{-3}	2132	7.534×10^{-3}	6.680×10^{-3}
-132.03	4.123×10^{-3}	1237	4.448×10^{-3}	3.798×10^{-3}
-131.53	2.190×10^{-3}	657	2.427×10^{-3}	1.953×10^{-3}
-131.03	1.050×10^{-3}	315	1.214×10^{-3}	8.860×10^{-4}
-130.53	5.730×10^{-4}	1719	6.113×10^{-4}	5.347×10^{-4}
-130.03	2.745×10^{-4}	549	3.070×10^{-4}	2.420×10^{-4}
-129.53	1.200×10^{-4}	240	1.415×10^{-4}	9.853×10^{-5}
-129.03	4.950×10^{-5}	198	5.925×10^{-5}	3.975×10^{-5}
-128.53	1.740×10^{-5}	348	1.999×10^{-5}	1.481×10^{-5}
-128.03	5.833×10^{-6}	175	7.055×10^{-6}	4.611×10^{-6}
-127.53	2.110×10^{-6}	183	2.542×10^{-6}	1.678×10^{-6}
-127.03	7.400×10^{-7}	74	9.784×10^{-7}	5.016×10^{-7}

TABLE 5

BIT ERROR RATE MEASUREMENTS

Data Rate = 300 b/s

Sequence Length = 2^6-1

P_{Signal}	$\hat{p}$	c	$U_{.95}$	$L_{.95}$
-138.16	7.065×10^{-3}	1413	7.586×10^{-3}	6.544×10^{-3}
-137.76	5.080×10^{-3}	1016	5.522×10^{-3}	4.638×10^{-3}
-137.56	3.700×10^{-3}	1480	3.967×10^{-3}	3.433×10^{-3}
-137.36	2.950×10^{-3}	885	3.225×10^{-3}	2.675×10^{-3}
-137.16	1.935×10^{-3}	387	2.208×10^{-3}	1.662×10^{-3}
-136.96	1.583×10^{-3}	475	1.784×10^{-3}	1.382×10^{-3}
-136.75	7.780×10^{-4}	778	8.553×10^{-4}	7.007×10^{-4}
-136.25	3.140×10^{-4}	314	3.631×10^{-4}	2.649×10^{-4}
-135.75	1.370×10^{-4}	137	1.694×10^{-4}	1.046×10^{-4}
-135.25	7.500×10^{-5}	119	9.406×10^{-5}	5.594×10^{-5}
-134.75	2.063×10^{-5}	166	2.507×10^{-5}	1.619×10^{-5}
-134.25	4.573×10^{-6}	69	6.099×10^{-6}	3.047×10^{-6}
-133.53	6.431×10^{-6}	163	7.827×10^{-6}	5.035×10^{-6}

TABLE 6

BIT ERROR RATE MEASUREMENTS

Data Rate = 75 b/s

Sequence Length = 2^6-1

P_{Signal}	$\hat{p}$	c	$U_{.95}$	$L_{.95}$
-143.6	3.480×10^{-3}	174	4.211×10^{-3}	2.749×10^{-3}
-143.1	1.390×10^{-3}	418	1.578×10^{-3}	1.202×10^{-3}
-142.6	7.036×10^{-4}	774	7.737×10^{-4}	6.335×10^{-4}
-142.1	2.920×10^{-4}	1168	3.157×10^{-4}	2.683×10^{-4}
-141.6	1.060×10^{-4}	636	1.177×10^{-4}	9.435×10^{-5}
-141.1	3.500×10^{-5}	210	4.169×10^{-5}	2.831×10^{-5}
-140.6	1.103×10^{-5}	64	1.485×10^{-5}	7.208×10^{-6}

TABLE 7

BIT ERROR RATE MEASUREMENTS

Data Rate = 9600 b/s

Sequence Length = $2^{20}-1$

P_{Signal}	$\hat{p}$	c	$U_{.95}$	$L_{.95}$
-128.25	1.179×10^{-1}	3537	1.234×10^{-1}	1.124×10^{-1}
-128.05	9.165×10^{-2}	3666	9.585×10^{-2}	8.745×10^{-2}
-127.75	6.673×10^{-2}	2669	7.031×10^{-2}	6.315×10^{-2}
-127.45	5.553×10^{-2}	2221	5.880×10^{-2}	5.226×10^{-2}
-127.25	5.378×10^{-2}	2151	5.699×10^{-2}	5.057×10^{-2}
-127.05	4.588×10^{-2}	1835	4.885×10^{-2}	4.291×10^{-2}
-126.75	4.192×10^{-2}	2096	4.446×10^{-2}	3.938×10^{-2}
-126.45	3.798×10^{-2}	1519	4.068×10^{-2}	3.528×10^{-2}
-126.25	3.155×10^{-2}	1262	3.401×10^{-2}	2.909×10^{-2}
-126.05	2.825×10^{-2}	1130	3.058×10^{-2}	2.592×10^{-2}
-125.75	2.292×10^{-2}	1146	2.480×10^{-2}	2.104×10^{-2}
-125.45	1.816×10^{-2}	908	1.983×10^{-2}	1.649×10^{-2}
-125.25	1.812×10^{-2}	906	1.979×10^{-2}	1.645×10^{-2}
-125.05	1.381×10^{-2}	2761	1.454×10^{-2}	1.308×10^{-2}
-124.75	1.077×10^{-2}	2153	1.141×10^{-2}	1.013×10^{-2}
-124.45	8.033×10^{-3}	2410	8.487×10^{-3}	7.579×10^{-3}
-124.25	7.590×10^{-3}	2277	8.031×10^{-3}	7.149×10^{-3}
-124.05	5.737×10^{-3}	1721	6.120×10^{-3}	5.354×10^{-3}
-123.75	4.480×10^{-3}	1344	4.819×10^{-3}	4.141×10^{-3}
-123.45	2.957×10^{-3}	887	3.232×10^{-3}	2.682×10^{-3}
-123.25	2.550×10^{-3}	765	2.806×10^{-3}	2.294×10^{-3}
-123.05	2.006×10^{-3}	2006	2.130×10^{-3}	1.882×10^{-3}
-122.75	1.345×10^{-3}	2690	1.417×10^{-3}	1.273×10^{-3}
-122.45	8.437×10^{-4}	2531	8.902×10^{-4}	7.972×10^{-4}
-122125	7.063×10^{-4}	2119	7.488×10^{-4}	6.638×10^{-4}
-122.05	4.767×10^{-4}	1430	5.116×10^{-4}	4.418×10^{-4}
-121.75	3.133×10^{-4}	940	3.416×10^{-4}	2.850×10^{-4}
-121.55	2.448×10^{-4}	2448	2.585×10^{-4}	2.311×10^{-4}
-121.25	1.455×10^{-4}	1455	1.561×10^{-4}	1.349×10^{-4}
-120.75	6.700×10^{-5}	1340	7.207×10^{-5}	6.193×10^{-5}
-120.25	2.957×10^{-5}	887	3.232×10^{-5}	2.682×10^{-5}
-119.25	6.710×10^{-6}	671	7.428×10^{-6}	6.113×10^{-6}
-119.75	1.427×10^{-5}	428	1.618×10^{-5}	1.236×10^{-5}
-118.75	3.830×10^{-6}	766	4.214×10^{-6}	3.446×10^{-6}

TABLE 8

BIT ERROR RATE MEASUREMENTS

Data Rate = 4800 b/s

Sequence Length = $2^{20}-1$

P_{Signal}	$\hat{p}$	c	$U_{.95}$	$L_{.95}$
-131.25	1.110×10^{-1}	6658	1.148×10^{-1}	1.072×10^{-1}
-131.05	1.067×10^{-1}	6401	1.104×10^{-1}	1.030×10^{-1}
-130.75	7.532×10^{-2}	4519	7.843×10^{-2}	7.221×10^{-2}
-130.25	5.602×10^{-2}	3361	5.870×10^{-2}	5.334×10^{-2}
-129.75	4.477×10^{-2}	2686	4.716×10^{-2}	4.238×10^{-2}
-129.25	3.247×10^{-2}	1948	3.451×10^{-2}	3.043×10^{-2}
-128.75	2.228×10^{-2}	1337	2.397×10^{-2}	2.059×10^{-2}
-128.25	1.593×10^{-2}	956	1.736×10^{-2}	1.450×10^{-2}
-127.75	9.950×10^{-3}	597	1.108×10^{-2}	8.821×10^{-3}
-127.25	7.900×10^{-3}	474	8.906×10^{-3}	6.894×10^{-3}
-126.75	4.498×10^{-3}	2699	4.738×10^{-3}	4.258×10^{-3}
-126.25	2.518×10^{-3}	1511	2.698×10^{-3}	2.338×10^{-3}
-125.75	1.397×10^{-3}	838	1.531×10^{-3}	1.263×10^{-3}
-125.25	7.267×10^{-4}	436	8.232×10^{-4}	6.302×10^{-3}
-124.75	3.490×10^{-4}	1047	3.789×10^{-4}	3.191×10^{-4}
-124.25	1.547×10^{-4}	464	1.746×10^{-4}	1.348×10^{-4}
-123.75	8.300×10^{-5}	249	9.758×10^{-5}	6.842×10^{-5}
-123.25	4.575×10^{-5}	915	4.994×10^{-5}	4.156×10^{-5}
-122.75	1.920×10^{-5}	384	2.192×10^{-5}	1.648×10^{-5}
-121.75	5.890×10^{-6}	589	6.563×10^{-6}	5.217×10^{-6}
-120.75	1.490×10^{-6}	149	1.828×10^{-6}	1.152×10^{-6}

TABLE 9

BIT ERROR RATE MEASUREMENTS

Data Rate = 2400 b/s

Sequence Length = $2^{20}-1$

P_{Signal}	$\hat{p}$	c	$U_{.95}$	$L_{.95}$
-132.25	4.265×10^{-2}	853	4.670×10^{-2}	3.860×10^{-2}
-131.75	2.770×10^{-2}	831	3.036×10^{-2}	2.504×10^{-2}
-131.25	2.023×10^{-2}	809	2.220×10^{-2}	1.826×10^{-2}
-130.75	1.383×10^{-2}	2766	1.456×10^{-2}	1.310×10^{-2}
-130.25	9.110×10^{-3}	1822	9.702×10^{-3}	8.518×10^{-3}
-129.75	5.620×10^{-3}	1124	6.085×10^{-3}	5.155×10^{-3}
-129.25	3.257×10^{-3}	977	3.546×10^{-3}	2.968×10^{-3}
-128.75	1.895×10^{-3}	758	2.086×10^{-3}	1.704×10^{-3}
-128.25	9.020×10^{-4}	902	9.852×10^{-4}	8.188×10^{-4}
-127.75	4.965×10^{-4}	993	5.402×10^{-4}	4.528×10^{-4}
-127.25	2.303×10^{-4}	691	2.546×10^{-4}	2.060×10^{-4}
-126.75	1.317×10^{-4}	395	1.501×10^{-4}	1.133×10^{-4}
-126.25	6.730×10^{-5}	1346	7.238×10^{-5}	6.222×10^{-5}
-125.75	3.340×10^{-5}	668	3.698×10^{-5}	2.982×10^{-5}
-125.25	1.720×10^{-5}	344	1.977×10^{-5}	1.463×10^{-5}
-124.75	8.300×10^{-6}	166	1.009×10^{-5}	6.514×10^{-6}
-123.75	1.990×10^{-6}	199	2.381×10^{-6}	1.599×10^{-6}

TABLE 10

BIT ERROR RATE MEASUREMENTS

Data Rate = 1200 b/s

Sequence Length = $2^{20}-1$

P_{Signal}	$\hat{p}$	c	$U_{.95}$	$L_{.95}$
-132.53	7.880×10^{-3}	2364	8.329×10^{-3}	7.431×10^{-3}
-132.03	4.710×10^{-3}	2355	4.979×10^{-3}	4.441×10^{-3}
-131.53	2.600×10^{-3}	1300	2.800×10^{-3}	2.400×10^{-3}
-131.03	1.410×10^{-3}	705	1.557×10^{-3}	1.263×10^{-3}
-130.53	7.357×10^{-4}	2207	7.791×10^{-4}	6.923×10^{-4}
-130.03	3.903×10^{-4}	1171	4.219×10^{-4}	3.587×10^{-4}
-129.53	2.047×10^{-4}	614	2.276×10^{-4}	1.818×10^{-4}
-129.03	1.190×10^{-4}	357	1.365×10^{-4}	1.015×10^{-4}
-128.53	5.633×10^{-5}	338	6.482×10^{-5}	4.784×10^{-5}
-128.03	2.500×10^{-5}	250	2.938×10^{-5}	2.062×10^{-5}
-127.53	1.540×10^{-5}	154	1.884×10^{-5}	1.196×10^{-5}
-126.53	4.600×10^{-6}	92	5.929×10^{-6}	3.271×10^{-6}
-125.53	1.180×10^{-6}	80	1.546×10^{-6}	8.143×10^{-7}
-125.53	1.080×10^{-6}	90	1.396×10^{-6}	7.644×10^{-7}
-125.03	9.160×10^{-7}	95	1.176×10^{-6}	6.555×10^{-7}

TABLE 11

BIT ERROR RATE MEASUREMENTS

Data Rate = 300 b/s

Sequence Length = $2^{20}-1$

P_{Signal}	$\hat{p}$	c	$U_{.95}$	$L_{.95}$
-137.53	3.745×10^{-3}	1498	4.013×10^{-3}	3.477×10^{-3}
-137.03	1.920×10^{-3}	1344	2.065×10^{-3}	1.775×10^{-3}
-136.53	8.500×10^{-4}	1020	9.238×10^{-4}	7.762×10^{-4}
-136.03	4.566×10^{-4}	2283	4.831×10^{-4}	4.301×10^{-4}
-135.53	1.763×10^{-4}	2292	1.865×10^{-4}	1.661×10^{-4}
-135.03	8.843×10^{-5}	619	9.828×10^{-5}	7.858×10^{-5}
-134.53	3.433×10^{-5}	618	3.816×10^{-5}	3.050×10^{-5}
-133.53	6.967×10^{-6}	209	8.303×10^{-6}	5.631×10^{-6}
-132.53	5.400×10^{-7}	27	8.281×10^{-7}	2.519×10^{-7}

TABLE 12

BIT ERROR RATE MEASUREMENTS

Data Rate = 75 b/s

Sequence Length = $2^{20}-1$

P_{Signal}	$\hat{p}$	c	$U_{.95}$	$L_{.95}$
-143.1	1.935×10^{-3}	387	2.208×10^{-3}	1.662×10^{-3}
-142.6	7.617×10^{-4}	457	8.605×10^{-4}	6.629×10^{-4}
-142.1	3.650×10^{-4}	365	4.180×10^{-4}	3.120×10^{-4}
-141.6	1.463×10^{-4}	439	1.657×10^{-4}	1.269×10^{-4}
-141.1	5.533×10^{-5}	332	6.375×10^{-5}	4.691×10^{-5}
-140.6	2.637×10^{-5}	188	3.170×10^{-5}	2.104×10^{-5}
-140.1	9.195×10^{-6}	60	1.249×10^{-5}	5.905×10^{-6}

TABLE 13

BIT ERROR RATE MEASUREMENTS

AN/SSR-1 Signal on Channel 1

other channels resistively

terminated ("RLY")

P_{Signal}	$\hat{p}$	c	$U_{.95}$	$L_{.95}$
-130.75	4.617×10^{-2}	277	5.38×10^{-2}	3.848×10^{-2}
-129.75	1.129×10^{-2}	1581	1.208×10^{-2}	1.050×10^{-2}
-128.75	1.269×10^{-3}	2665	1.337×10^{-3}	1.201×10^{-3}
-127.80	2.500×10^{-5}	30	3.765×10^{-5}	1.235×10^{-5}

TABLE 14

AN/SSR-1 Signal on Channel 1

other channels not used ("OFF")

P_{Signal}	$\hat{p}$	c	$U_{.95}$	$L_{.95}$
-133.85	2.150×10^{-3}	1075	2.332×10^{-3}	1.968×10^{-3}
-132.85	8.660×10^{-3}	1732	9.237×10^{-3}	8.083×10^{-3}
-131.85	3.110×10^{-3}	622	3.456×10^{-3}	2.764×10^{-3}
-130.80	7.081×10^{-4}	2195	7.500×10^{-4}	6.662×10^{-4}
-129.80	1.117×10^{-4}	670	1.237×10^{-4}	9.974×10^{-5}
-128.75	1.125×10^{-5}	45	1.590×10^{-5}	6.601×10^{-6}

REFERENCES

1. Stein, S. and Jones, J., Modern Communications Principles, McGraw Hill, 1967.

2. Viterbi, A., Principles of Coherent Communications, p. 191-214, McGraw Hill, 1967.

3. Office of Telecommunications Report OTM 7451, Confidence Limits for Digital Error Rates, Crow, E., November 1974.

4. Jordan, E. and Balmain, K., Electromagnetic Waves and Radiating Systems, p. 416, Prentice-Hall, 1968.

5. Naval Electronics Systems Command ELEX-C-168, Communications Set, Satellite AN/WSC-3, Contract Specifications 4 December 1973.

6. Hewlett Packard Application Note 150-4, Spectrum Analysis Noise Measurements, p. 8, April 1974.

7. Commander Naval Electronics Systems Command Document No. 68-11198, Installation Test Set Part No. 01-P11140E001, Motorola, 10 October 1974.

INITIAL DISTRIBUTION LIST
(NPS-620L76102)

		No. of Copies
1.	Defense Documentation Center Cameron Station Alexandria, VA 22314	2
2.	Library, Code 0212 Naval Postgraduate School Monterey, CA 93940	2
3.	Dean of Research, Code 023 Naval Postgraduate School Monterey, CA 93940	1
4	Chairman, Code 62 Electrical Engineering Department Naval Postgraduate School Monterey, California	1
5.	Associate Professor J. E. Ohlson, Code 620L Naval Postgraduate School Monterey, CA 93940	25
6.	LCDR C. J. Waylan, Code PME 106-IT Naval Electronic Systems Command Washington, DC 20360	12
7.	Director (Attn: Dr. Steve Bernstein) M.I.T. Lincoln Laboratory P.O. Box 73 Lexington, MA 02173	1
8.	Dr. J. Geist Harris Electronic Systems Division P.O. Box 37 Melbourn, FL 32901	1
9.	Dr. P. McAdam Bldg. R6/1385 T.R.W. Inc. One Space Park Redondo Beach, CA 90278	1
10.	Director Naval Research Laboratory (Attn: Code 5400) Washington, DC 20375	1

		No. of Copies
11.	Commander Naval Electronics Laboratory Center (Attn: Code 1410) San Diego, CA 92152	1
12.	Commander Naval Electronics Laboratory Center (Attn: Ralph D. Jensen) San Diego, CA 92152)	1
13.	Motorola, Inc. (Attn: Robert Fitting) 8201 East McDowell Road Scottsdale, AZ 85252	1
14.	Commander Naval Electronic Systems Test and Evaluation Detachment Patuxent River, MD 20670	1
15.	NAVSEEACT (Attn: LCDR G. A. Burman) Box 194 FPO San Francisco 96630	1
16.	Commander Naval Electronic Systems Engineering Center Vallejo, California 94592	1
17.	Electronic Communications, Inc. 1501 - 72nd St. No., Box 12248 St. Petersburg, FL 33733	1
18.	LT Richard F. Carlson, USCG COMMANDANT (G-OTM-3) U.S. Coast Guard Washington, DC 20590	1
19.	Electromagnetic Compatibility Analysis Center (Attn: ACY) North Severn Annapolis, MD 21402	1
20.	Security Officer (Attn: C. D. McBiles, Mail Drop 1306) MOTOROLA, Inc. GED 8201 E. McDowell Road Scottsdale, AZ 85252	1

No. of copies

21. Director — 1
(Attn: D. H. Townsend, Code 5435)
Naval Research Laboratory
Washington, DC 20375

22. Commander — 1
(Attn: R. S. Trible, 0252)
NESTED
Patuxent River, MD 20670

23. Commander — 1
Naval Electronic Systems Command
(Attn: Mortun Runey, ELEX 952)
Washington, DC 20360

24. Security Officer — 1
(Attn: A. H. Ballard)
TRW Systems, Washington Operations
9600 Colshire Drive
McLean, VA 22101

25. Commander — 1
(Attn: S. Caine, Elex 51024)
Naval Electronic Systems Command
Washington, DC 20360

26. Commander — 1
(Attn: CDR R. R. Grove, SEA 06T)
Naval Sea Systems Command
Washington, DC 20360

27. William C. Lindsey — 1
Powell Hall 524
Department of Electrical Engineering
University of Southern California
Los Angeles, CA 90007

28. Commander — 1
(Attn: H. J. Buhl, Elex 51013)
Naval Electronics System Command
Washington, DC 20360